

ELECTRONIC SUPPORTING INFORMATION

Formation of Supported Rhodium Clusters from Mononuclear Rhodium Complexes Controlled by the Support and Ligands on Rhodium

*Pedro Serna, Dicle Yardimci, Joseph D. Kistler, and Bruce. C. Gates**

EXAFS Data Analysis: The X-ray absorption edge energy was calibrated with the measured signal of rhodium metal foil scanned at the Rh K edge, which was taken to be the inflection point at 23220 eV. The data were normalized by dividing the absorption intensity by the height of the absorption edge. Analysis of the EXAFS data was carried out with the software ATHENA of the IFEFFIT¹ package and the software XDAP.² ATHENA was used for edge calibration, deglitching, data normalization, and conversion of the data into an EXAFS (chi) file. A background function was subtracted from the normalized data by using spline points between the values of the wave vector (k) of 2.5 and 14.2 Å⁻¹, with a strong spline clamp made to the end point. The k -weighting for the background removal was set to be 2 for all spectra. XDAP allowed the efficient application of a “difference-file” technique³ for determination of optimized fit parameters.

Structural models postulated for the supported rhodium species were compared with the EXAFS data; the models included the plausible contributions. Reference files, with backscattering amplitudes and phase shifts for the various contributions, were calculated with the software FEFF 7.0⁴ from crystallographic coordinates of the unit cells of the reference compounds rhodium metal, Rh(C₂H₄)₂(acac), Rh(CO)₂(acac), Rh₂MgO₄, And Rh-Al alloy. Data analysis was carried out with unfiltered data; iterative fitting was performed until optimum agreement was attained between the calculated k^0 -, k^1 -, k^2 -, and k^3 -weighted EXAFS data and each postulated model. The data were fitted in r space with the Fourier-transformed chi data (r is the distance from the absorbing atom; chi is the EXAFS function). The EXAFS data were analyzed with a maximum of 20 free parameters over the ranges $2.5 < k < 15.0$ Å⁻¹ and $0.8 < r < 3.5$ Å. The k -ranges were determined conventionally³ at the low end by where the background could be reliably separated from the total absorption and at the high end by where the signal became difficult to distinguish from the noise.⁵ The R (distance) ranges were determined as recommended⁵ in the “difference file” method by considering each shell individually and including the full range for each such that it included the full range over which a satisfactory fit could be obtained for each individual shell. To estimate the error in the data, the root mean square of the value obtained from the subtraction of smoothed chi data from the background-subtracted experimental values was calculated and used for the calculation the goodness of fit according to the following expression:

$$\text{goodness of fit} = \frac{\nu}{NPTS(\nu - N_{free})} \sum_{i=1}^{NPTS} \left(\frac{\chi_{\text{exp},i} - \chi_{\text{model},i}}{\sigma_{\text{exp},i}} \right)^2$$

where χ_{model} and χ_{exp} are the fit and experimental EXAFS respectively, σ_{exp} is the error in the experimental results, ν is the number of independent data points in the fit range, and NPTS is the actual number of data points in the fit range.

The approximate accuracies of the fit parameters characterizing the absorber-backscatterer pair contributions are estimated to be as follows (with a caveat, stated below): coordination number N , $\pm 20\%$; distance R , $\pm 2\%$ Å; Debye–Waller factor $\Delta\sigma^2$, $\pm 20\%$; and inner potential correction ΔE_0 , $\pm 20\%$. The number of parameters used in the fitting was always less than the statistically justified number, computed with the Nyquist theorem:⁶ $n = (2\Delta k\Delta r/\pi) + 2$, where Δk and Δr , respectively, are the k and r ranges used in the fitting. For efficiency in the data reduction, the most thorough EXAFS analyses were done for key samples and treatments to provide starting points; then quicker, less thorough analyses were done by interpolation for the samples with intermediate structures that formed during the transformations. The caveat is that the errors in the Rh–Mg and Rh–Al contributions are larger than those characterizing the other contributions, and a basis for estimates of the uncertainties in these values is not provided by the data.

Table S1. EXAFS fit parameters^a characterizing supported rhodium species at the Rh K edge: (1) Sample 1 was formed by adsorption of Rh(C₂H₄)₂(acac) on MgO ($\Delta k = 3.8\text{--}13.3 \text{ \AA}^{-1}$, $\Delta R = 0.8\text{--}3.7 \text{ \AA}$); (2) Sample 2 was formed by adsorption of Rh(C₂H₄)₂(acac) on zeolite HY ($\Delta k = 3.7\text{--}12.8 \text{ \AA}^{-1}$, $\Delta R = 0.8\text{--}3.8 \text{ \AA}$); (3) Sample 3 was formed by adsorption of Rh(CO)₂(acac) on MgO ($\Delta k = 2.7\text{--}12.3 \text{ \AA}^{-1}$, $\Delta R = 0.8\text{--}4.0 \text{ \AA}$); (4) Sample 4 was formed by adsorption of Rh(CO)₂(acac) on zeolite HY ($\Delta k = 3.4\text{--}11.3 \text{ \AA}^{-1}$, $\Delta R = 0.8\text{--}4.0 \text{ \AA}$).^{1,2}

Sample	Shell	<i>N</i>	<i>R</i> (Å)	10 ³ × Δσ ² (Å ²)	Δ <i>E</i> ₀ (eV)
1 ¹	Rh–Rh	-	-	-	-
	Rh–C _{ethene}	4.0	2.06	1.32	2.7
	Rh–O _{support}	2.2	2.15	1.75	-5.1
	Rh–Mg	1.2	3.09	3.51	3.8
2	Rh–Rh	-	-	-	-
	Rh–C _{ethene}	3.7	2.08	3.80	3.8
	Rh–O _{support}	2.1	2.15	3.10	7.1
	Rh–Al	1.1	3.02	6.70	-2.5
3 ¹	Rh–Rh	-	-	-	-
	Rh–C _{Oterminal}	2.2	2.08	1.15	-1.1
	Rh–O _{Cterminal}	2.1	3.06	3.75	-7.6
	Rh–O _{support}	2.0	2.13	3.71	2.7
	Rh–Mg	1.2	3.19	0.01	-2.4
4 ²	Rh–Rh	-	-	-	-
	Rh–O _{support}	2.0	2.10	4.44	7.2
	Rh–C _{Oterminal}	1.9	1.86	5.37	7.8
	Rh–O _{Cterminal}	1.9	3.01	1.59	-6.0
	Rh–Al	0.9	3.20	0.10	-7.7

^aNotation: *N*, coordination number; *R*, distance between absorber and backscatterer atoms; Δσ², disorder term; Δ*E*₀, inner potential correction. Error bounds (accuracies) characterizing the structural parameters obtained by EXAFS spectroscopy are estimated to be as follows: *N*, ±20%; *R*, ±0.02 Å; Δσ², ±20%; and Δ*E*₀, ±20 (but see that caveat stated above). Sources: ¹Yardimci, D.; Serna, P.; Gates, B. C., *Chem. Eur. J.* **2013**, *19/4*, 1235–1245. ²Yardimci, D.; Serna, P.; Gates, B. C., *ACS Catal.* **2012**, *2*, 2100–2113.

Table S2. EXAFS fit parameters characterizing a rhodium foil at the rhodium K edge
 ($\Delta k = 2.6\text{--}14.8 \text{ \AA}^{-1}$, $\Delta R = 1.0\text{--}3.2 \text{ \AA}$)

Sample	Shell	N	R (\AA)	$10^3 \times \Delta\sigma^2$ (\AA^2)	ΔE_0 (eV)
Rh Foil	Rh–Rh	12.0	2.68	6.41	6.1

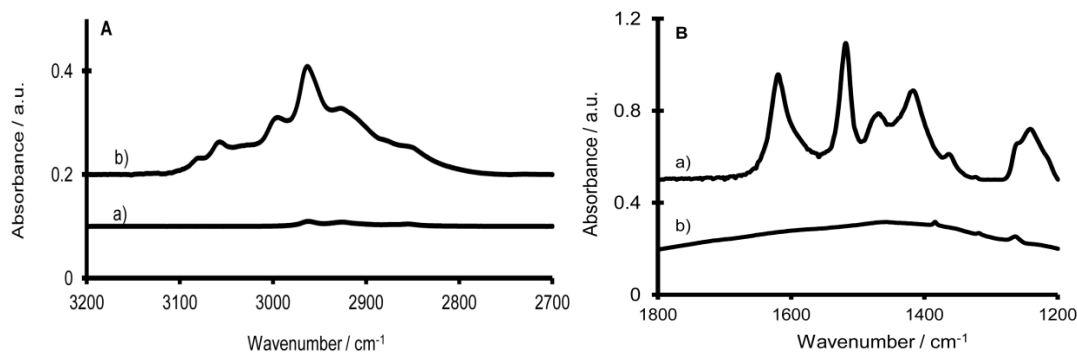


Fig. S1. IR spectra characterizing the C–H stretching region (A) and the 1800–1200 cm^{-1} region (B) of the following samples (in helium at 298 K and 1 bar): a) highly dehydroxylated MgO and b) highly dehydroxylated MgO after adsorption of $\text{Rh}(\text{C}_2\text{H}_4)_2(\text{acac})$ at 298 K. The bands at 3059 and 2999 cm^{-1} (A), which are ascribed to π -bonded ethylene, indicate that the ethylene ligands were still bonded to the rhodium atom after adsorption of the rhodium complex on MgO. The bands at 1621, 1520, 1467, 1417, 1362, and 1262 cm^{-1} (B), which appeared after adsorption

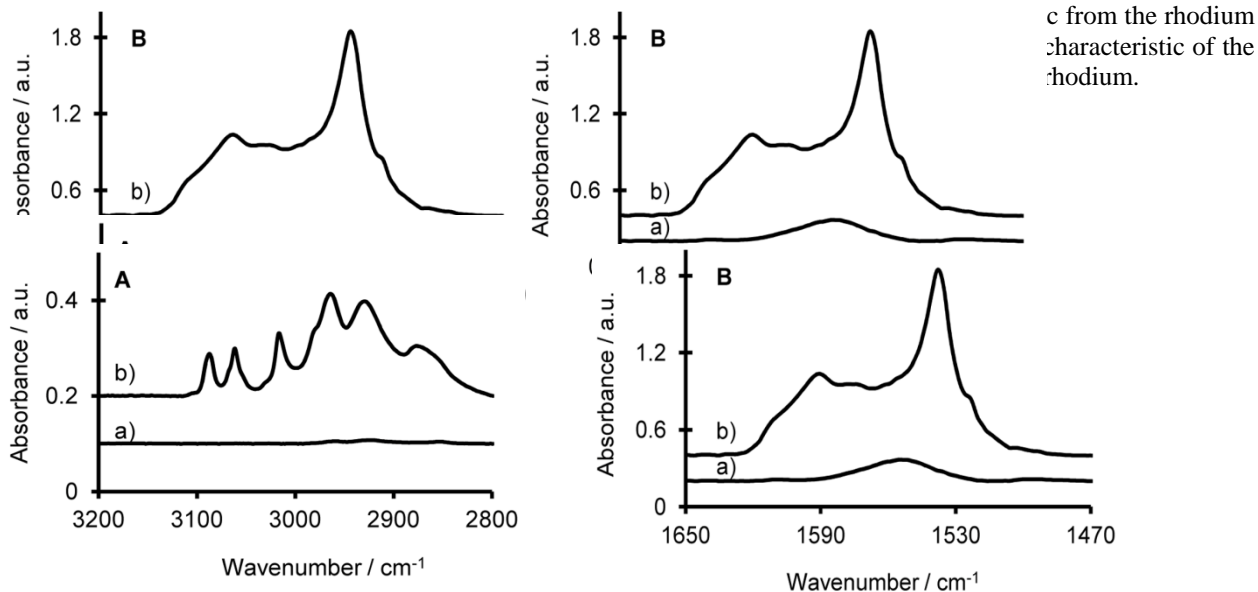


Fig. S2. IR spectra characterizing the C–H stretching region (A) and the 1650–1470 cm^{-1} region (B) of the following samples (in helium at 298 K and 1 bar): a) zeolite HY, and b) zeolite HY after adsorption of $\text{Rh}(\text{C}_2\text{H}_4)_2(\text{acac})$ at 298 K.

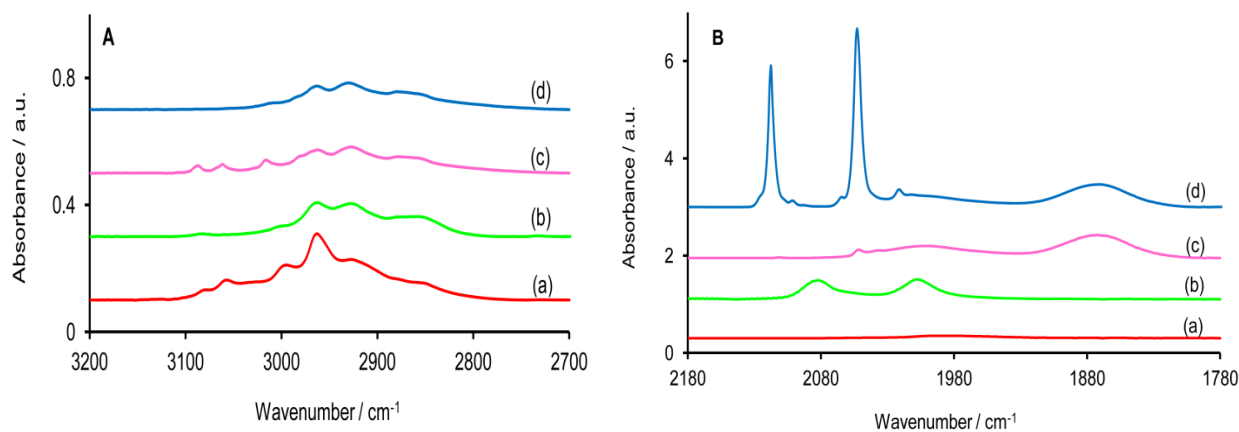


Fig. S3. IR spectra characterizing the C–H stretching region (A) and C–O stretching region (B) of the following samples: MgO-supported Rh(C₂H₄)₂ complexes in helium at 298 K and 1 bar (a); sample represented by spectrum (a) exposed to a pulse of CO in helium at 298 K and 1 bar (b); zeolite HY-supported Rh(C₂H₄)₂ complexes in helium at 298 K and 1 bar (c); sample represented by spectrum (c) after exposure to a pulse of CO in helium at 298 K and 1 bar (d).

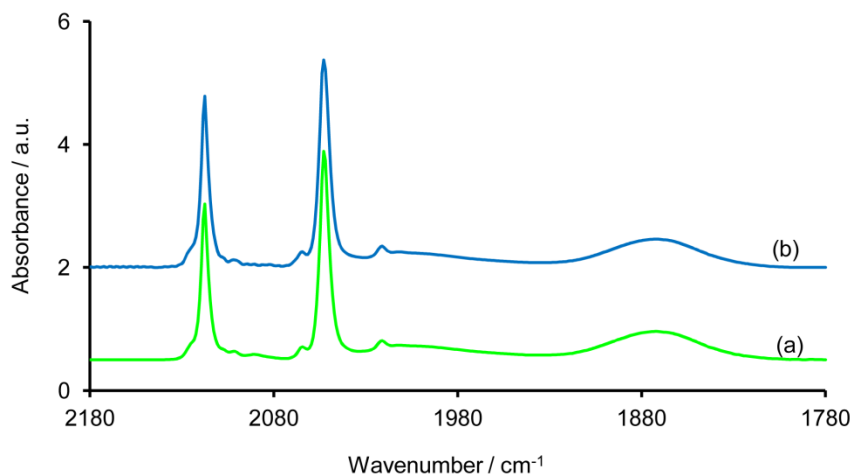


Fig. S4. IR spectra characterizing the CO stretching region of the following samples: zeolite HY-supported Rh(CO)₂ complexes in helium at 298 K and 1 bar (a); sample (a) treated in H₂ at 423 K and 1 bar (b).

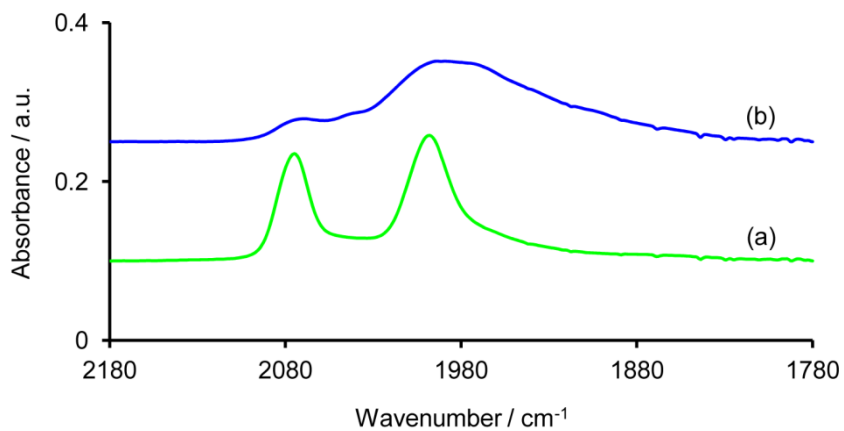


Fig. S5. IR spectra characterizing the CO stretching region of the following samples: MgO-supported Rh(CO)₂ complexes in helium at 298 K and 1 bar (a); sample (a) after treatment in H₂ at 393 K and 1 bar (b).

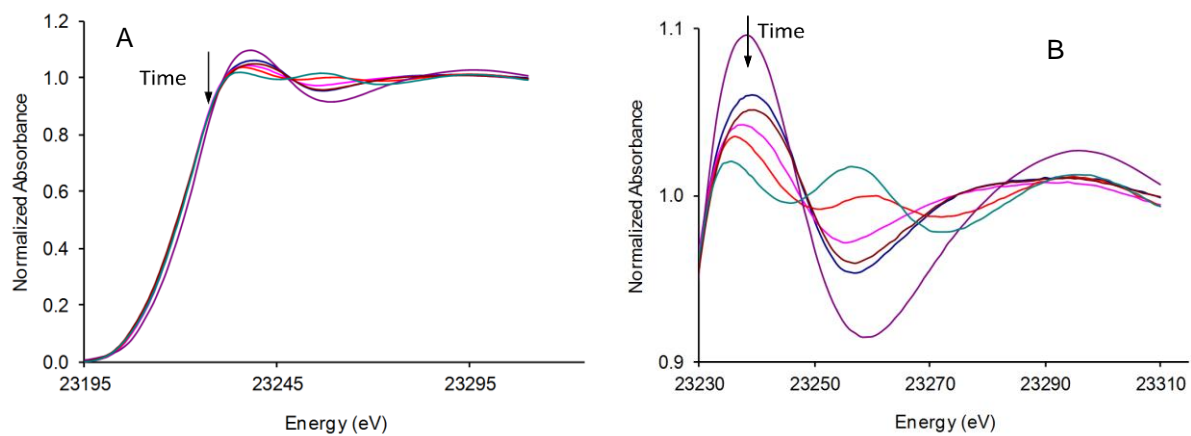


Fig. S6. Normalized XANES spectra at the Rh K edge characterizing the samples during cluster formation from $\text{Rh}(\text{C}_2\text{H}_4)_2$ complexes supported on zeolite HY at 298 K with the sample in flowing H_2 at 1 bar. Figure B shows a zoomed-in image of the region near the white line, showing that the various curves do not cross at isosbestic points.

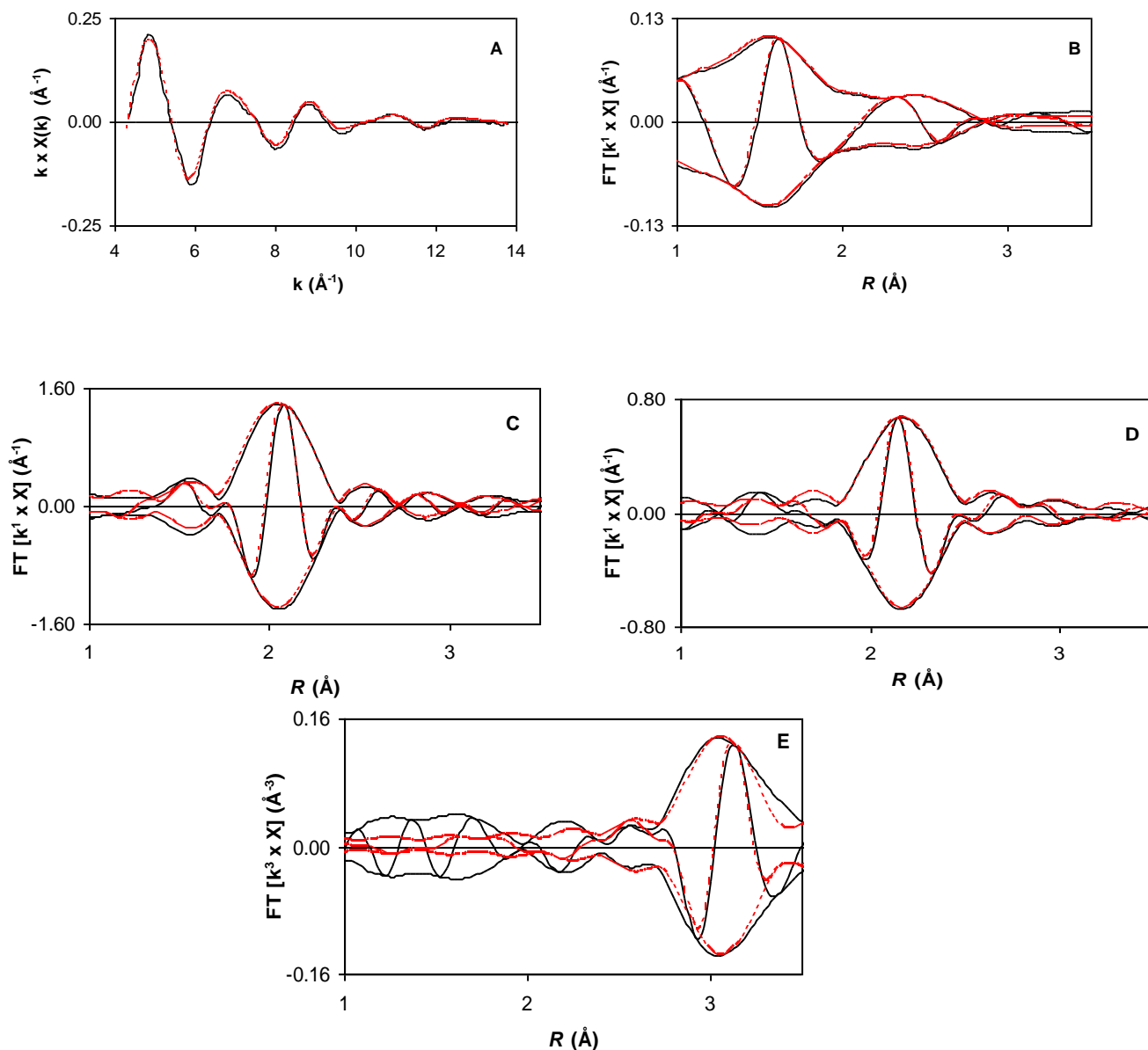


Fig. S7. EXAFS data recorded at the Rh K edge characterizing the supported sample prepared by adsorption of $\text{Rh}(\text{C}_2\text{H}_4)_2(\text{acac})$ on highly dehydroxylated MgO (Table S1, sample 1): (A) k^1 -Weighted EXAFS function, $k^1(\chi)$ (solid line) and sum of the calculated contributions (dashed line). (B) k^1 -Weighted imaginary part and magnitude of the Fourier transform of data (solid line) and sum of the calculated contributions (dashed line). (C) k^1 -Weighted, phase- and amplitude-corrected, imaginary part and magnitude of the Fourier transform of data (solid line) and calculated contributions (dashed line) of Rh–C shell. (D) k^1 -Weighted, phase- and amplitude-corrected, imaginary part and magnitude of the Fourier transform of data (solid line) and calculated contributions (dashed line) of Rh–O shell. (E) k^3 -Weighted, phase- and amplitude-corrected, imaginary part and magnitude of the Fourier transform of data (solid line) and calculated contributions (dashed line) of Rh–Mg shell ($\Delta k = 3.8\text{--}13.3 \text{ \AA}^{-1}$). The approximate experimental uncertainties are as follows: coordination number N , $\pm 20\%$; R , $\pm 0.02 \text{ \AA}$; $\Delta\sigma^2$, $\pm 20\%$; and ΔE_0 , $\pm 20\%$.

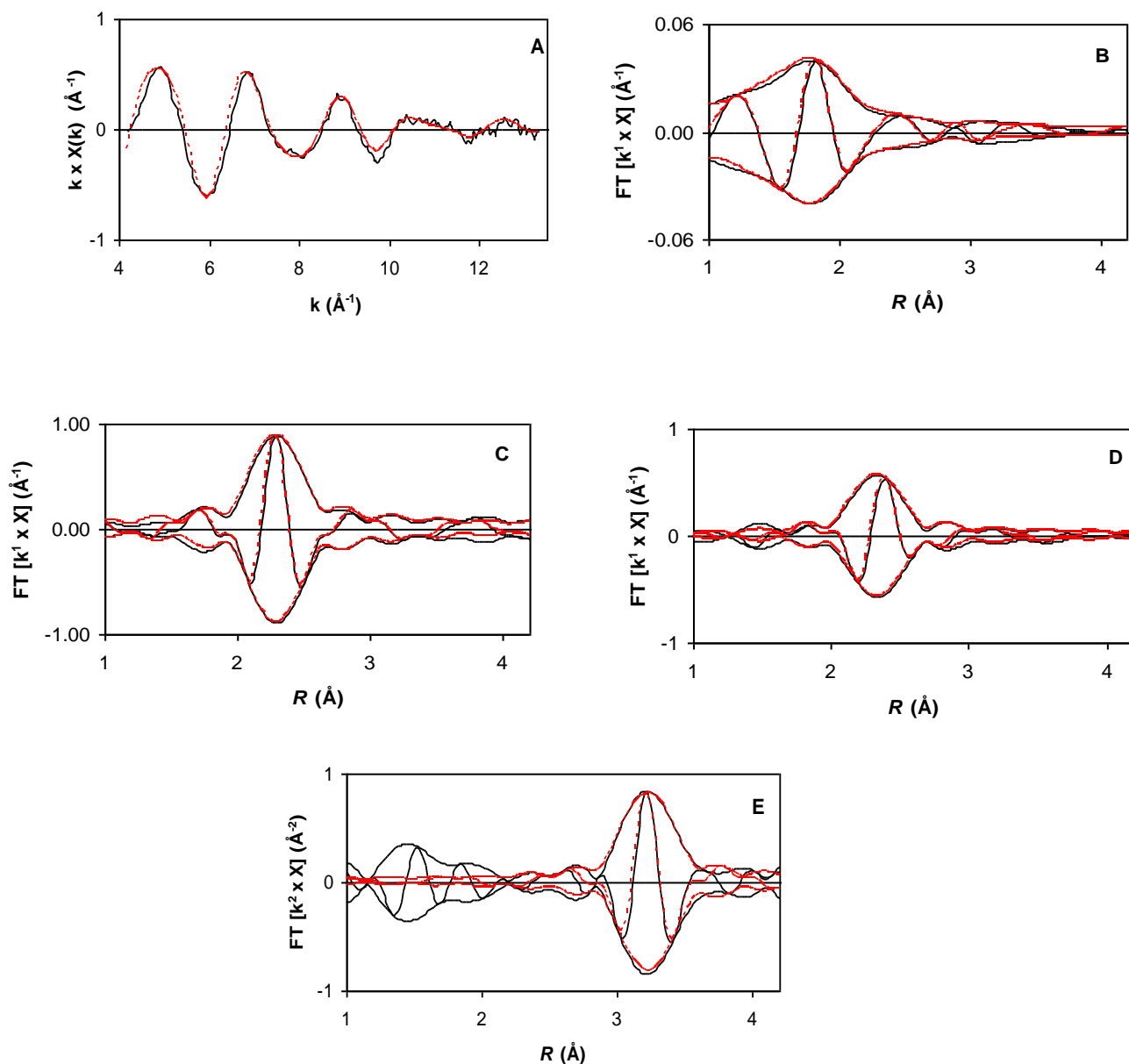
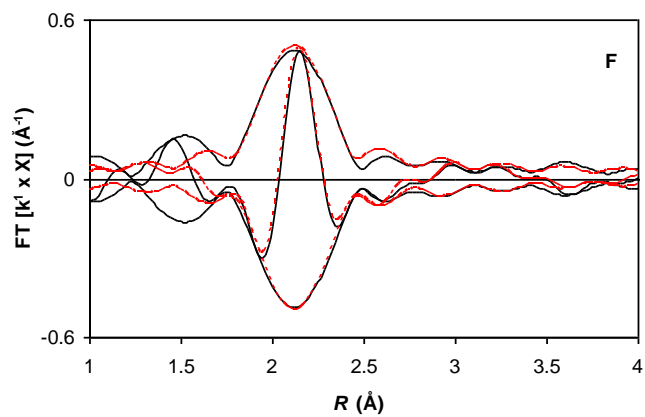
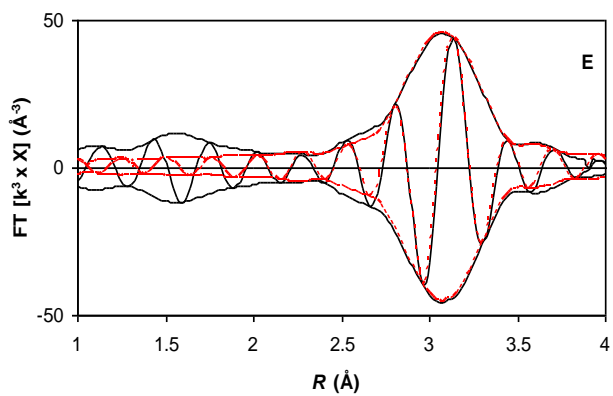
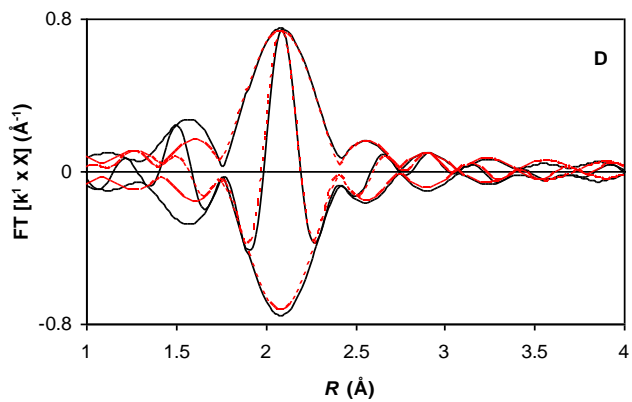
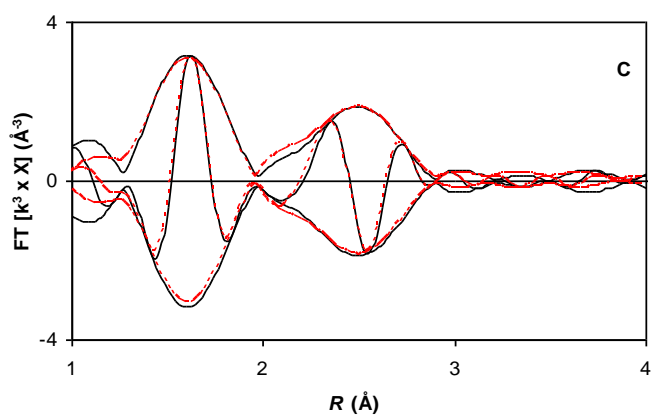
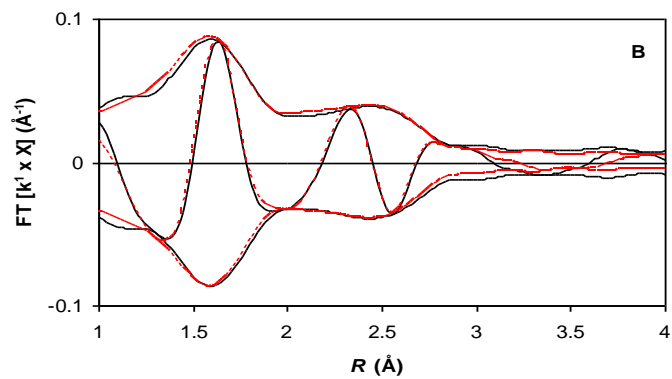
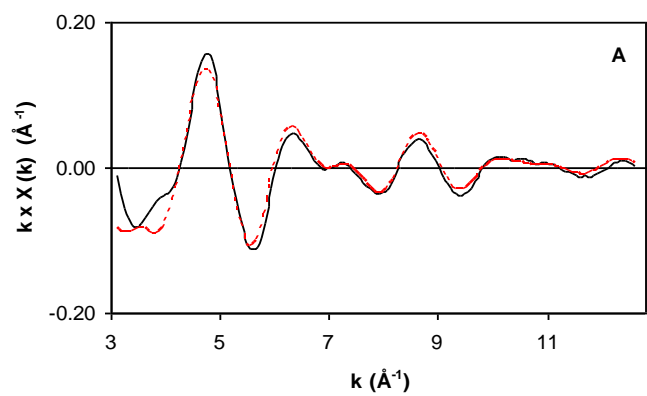


Fig. S8. EXAFS data recorded at the Rh K edge characterizing the supported sample prepared by adsorption of $\text{Rh}(\text{C}_2\text{H}_4)_2(\text{acac})$ on the zeolite HY (Table S1, Sample 2): (A) k^1 -Weighted EXAFS function, $k^1(\chi)$ (solid line) and sum of the calculated contributions (dashed line). (B) k^1 -Weighted imaginary part and magnitude of the Fourier transform of data (solid line) and sum of the calculated contributions (dashed line). (C) k^1 -Weighted, phase- and amplitude-corrected, imaginary part and magnitude of the Fourier Transform of data (solid line) and calculated contributions (dashed line) of Rh–C_{ethene} shell. (D) k^1 -Weighted, phase- and amplitude-corrected, imaginary part and magnitude of the Fourier transform of data (solid line) and calculated contributions (dashed line) of Rh–O_{support} shell. (E) k^2 -Weighted, phase- and amplitude-corrected, imaginary part and magnitude of the Fourier transform of data (solid line) and calculated contributions (dashed line) of Rh–Al shell ($\Delta k = 3.7\text{--}12.8 \text{ \AA}^{-1}$). The approximate experimental uncertainties are as follows: coordination number N , $\pm 20\%$; R , $\pm 0.02 \text{ \AA}$; $\Delta\sigma^2$, $\pm 20\%$; and ΔE_0 , $\pm 20\%$ (but see the caveat stated above on page SI-3).



continued on next page

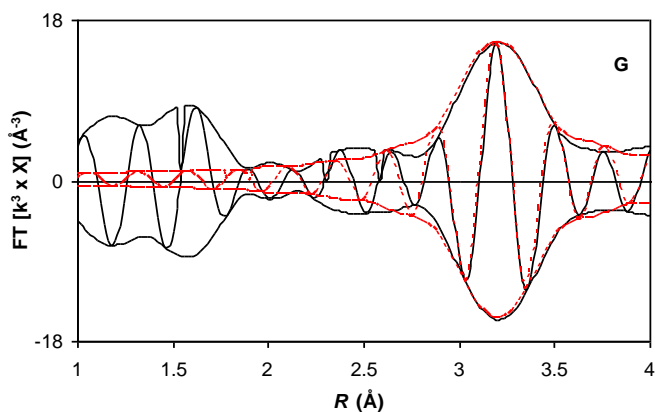
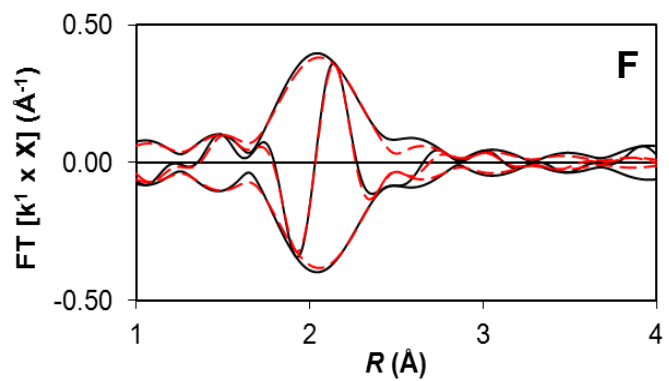
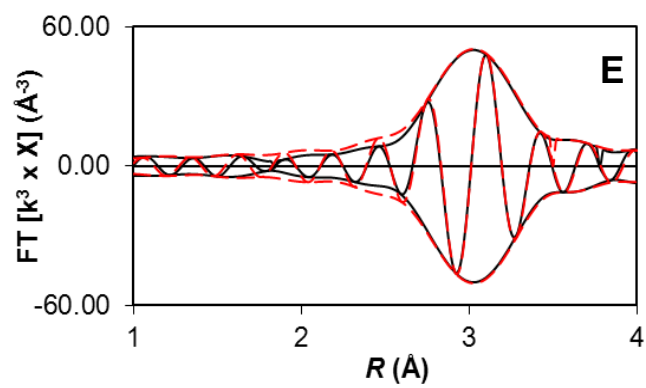
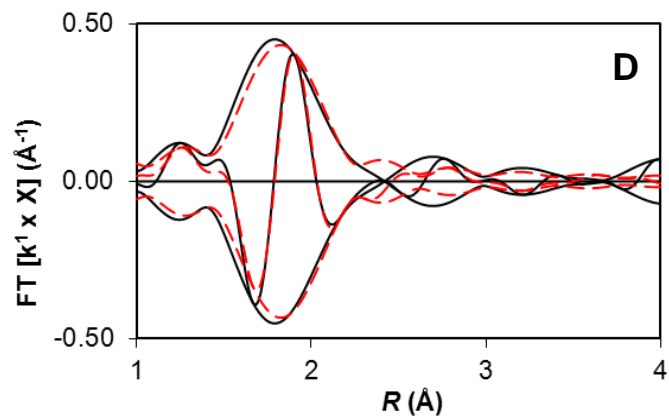
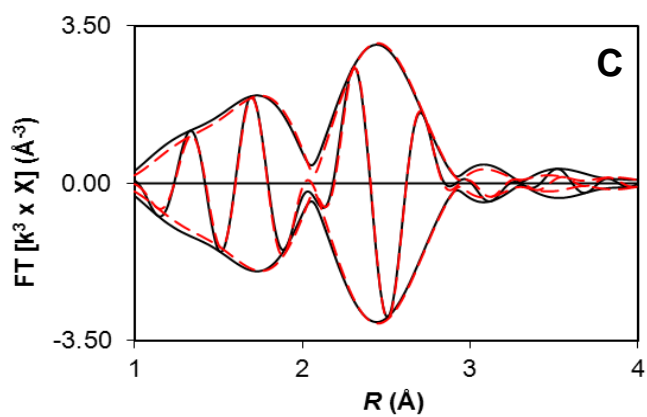
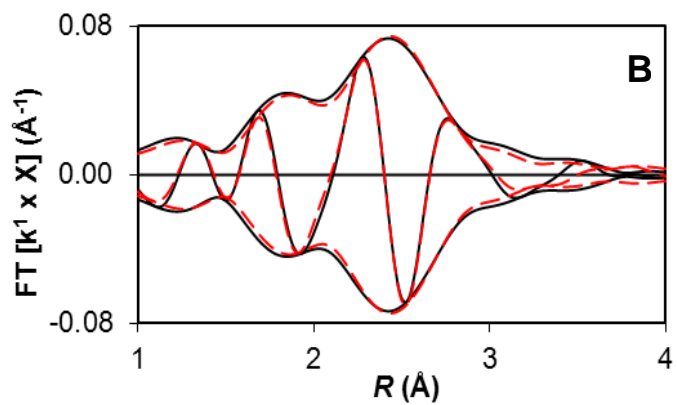
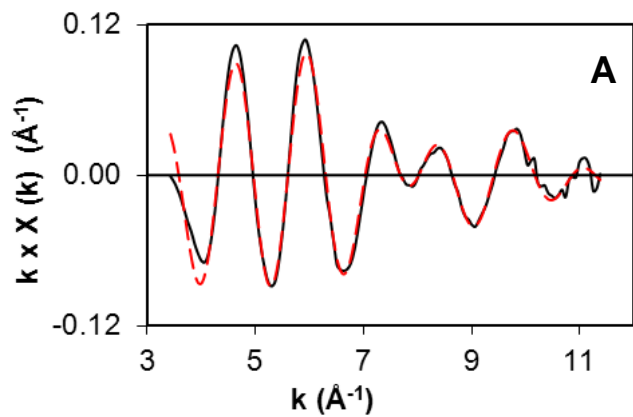


Fig. S9. EXAFS data recorded at the Rh K edge characterizing sample formed by adsorption of $\text{Rh}(\text{C}_2\text{H}_4)_2(\text{acac})$ on highly dehydroxylated MgO after treatment with a pulse of CO for 1 min at 298 K and 1 bar to form $\text{Rh}(\text{CO})_2$ species on MgO (Table S1, sample 3): (A) k^1 -Weighted EXAFS function, $k^1(\chi)$ (solid line) and sum of the calculated contributions (dashed line). (B) k^1 -Weighted imaginary part and magnitude of the Fourier transform of data (solid line) and sum of the calculated contributions (dashed line). (C) k^3 -Weighted imaginary part and magnitude of the Fourier transform of data (solid line) and sum of the calculated contributions (dashed line). (D) k^1 -Weighted, phase- and amplitude-corrected, imaginary part and magnitude of the Fourier transform of data (solid line) and calculated contributions (dashed line) of Rh-C_{co} shell. (E) k^3 -Weighted, phase- and amplitude-corrected, imaginary part and magnitude of the Fourier transform of data (solid line) and calculated contributions (dashed line) of Rh-O_{co} shell. (F) k^1 -Weighted, phase- and amplitude-corrected, imaginary part and magnitude of the Fourier transform of data (solid line) and calculated contributions (dashed line) of Rh-O_{support} shell. (G) k^3 -Weighted, phase- and amplitude-corrected, imaginary part and magnitude of the Fourier transform of data (solid line) and calculated contributions (dashed line) of Rh-Mg shell ($\Delta k = 2.7\text{--}12.3 \text{ \AA}^{-1}$). The approximate experimental uncertainties are as follows: coordination number N , $\pm 20\%$; R , $\pm 0.02 \text{ \AA}$; $\Delta\sigma^2$, $\pm 20\%$; and ΔE_0 , $\pm 20\%$ (but see the caveat stated above on page SI-3).



continued on next page

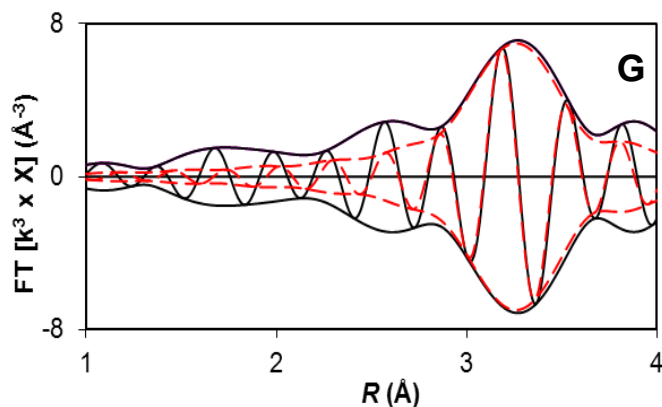
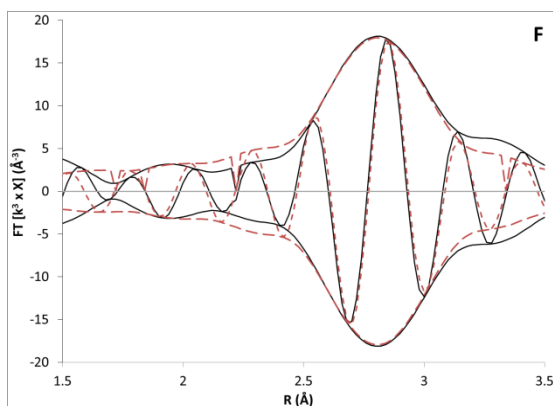
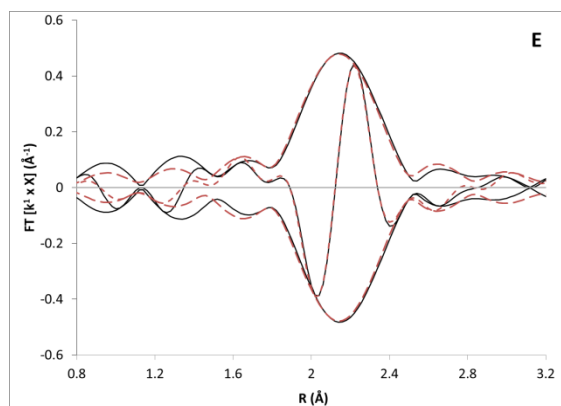
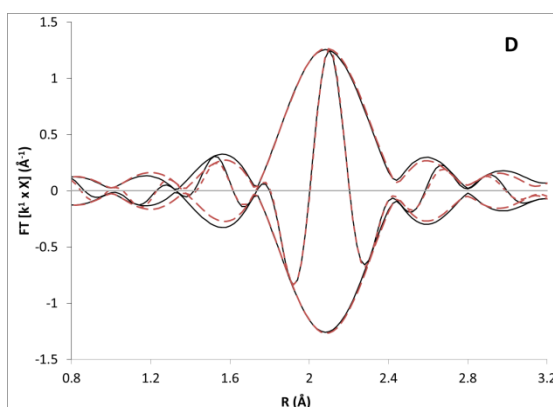
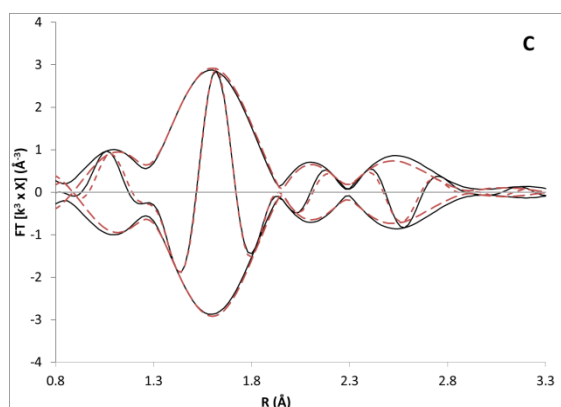
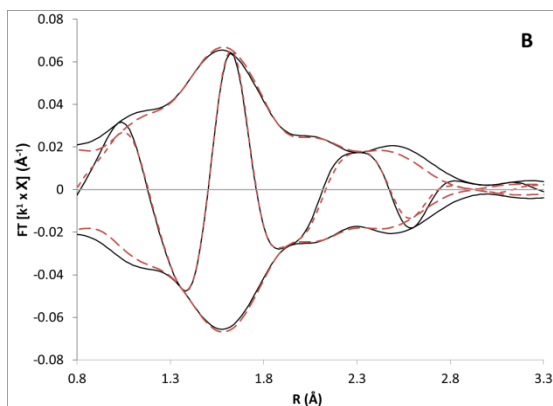
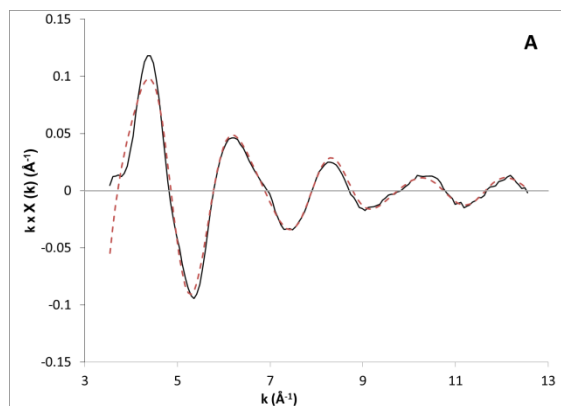


Fig. S10. EXAFS data recorded at the Rh K edge characterizing sample formed by adsorption of $\text{Rh}(\text{C}_2\text{H}_4)_2(\text{acac})$ on zeolite HY after treatment with a pulse of CO for 1 min at 298 K and 1 bar to form $\text{Rh}(\text{CO})_2$ species on zeolite HY (Table S1, sample 4): (A) k^1 -Weighted EXAFS function, $k^1(\chi)$ (solid line) and sum of the calculated contributions (dashed line). (B) k^1 -Weighted imaginary part and magnitude of the Fourier transform of data (solid line) and sum of the calculated contributions (dashed line). (C) k^3 -Weighted imaginary part and magnitude of the Fourier transform of data (solid line) and sum of the calculated contributions (dashed line). (D) k^1 -Weighted, phase- and amplitude-corrected, imaginary part and magnitude of the Fourier transform of data (solid line) and calculated contributions (dashed line) of Rh-C_{co} shell. (E) k^3 -Weighted, phase- and amplitude-corrected, imaginary part and magnitude of the Fourier transform of data (solid line) and calculated contributions (dashed line) of Rh-O_{co} shell. (F) k^1 -Weighted, phase- and amplitude-corrected, imaginary part and magnitude of the Fourier transform of data (solid line) and calculated contributions (dashed line) of Rh-O_{support} shell. (G) k^3 -Weighted, phase- and amplitude-corrected, imaginary part and magnitude of the Fourier transform of data (solid line) and calculated contributions (dashed line) of Rh-Al shell ($\Delta k = 3.4\text{--}11.3 \text{ \AA}^{-1}$). The approximate experimental uncertainties are as follows: coordination number N , $\pm 20\%$; R , $\pm 0.02 \text{ \AA}$; $\Delta\sigma^2$, $\pm 20\%$; and ΔE_0 , $\pm 20\%$ (but see the caveat stated above on page SI-3).



continued on next page

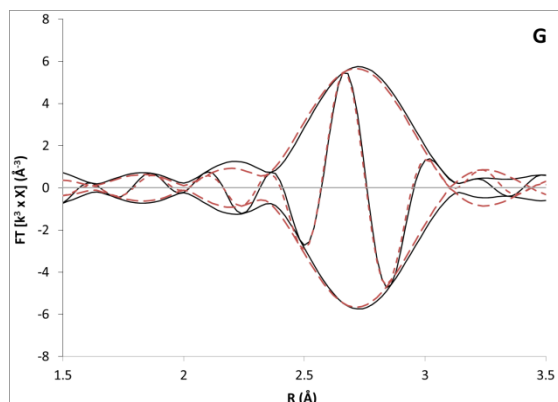
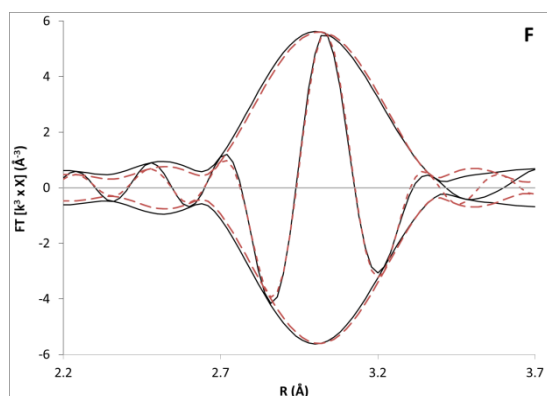
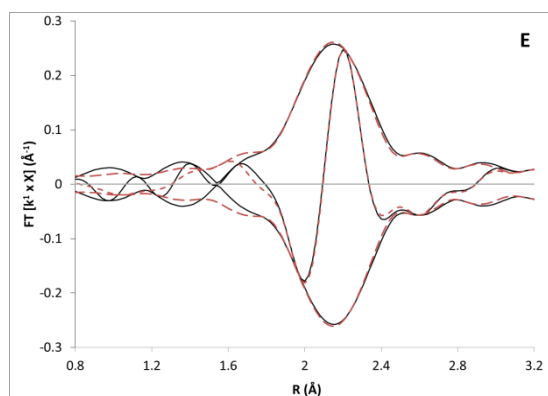
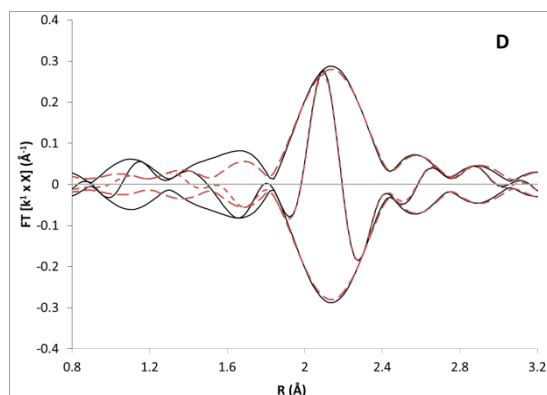
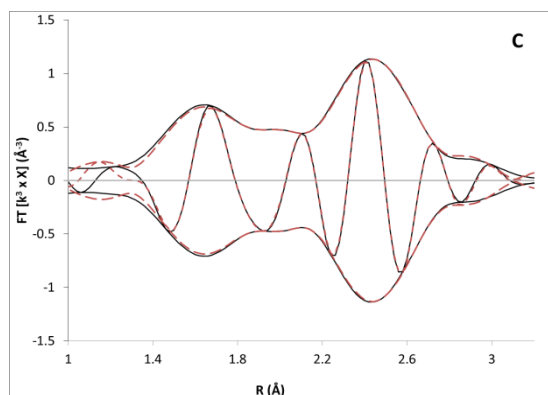
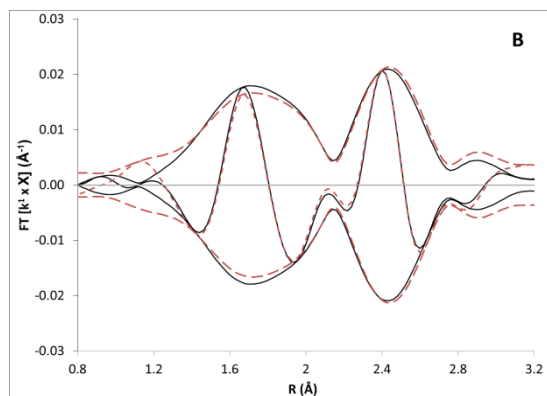
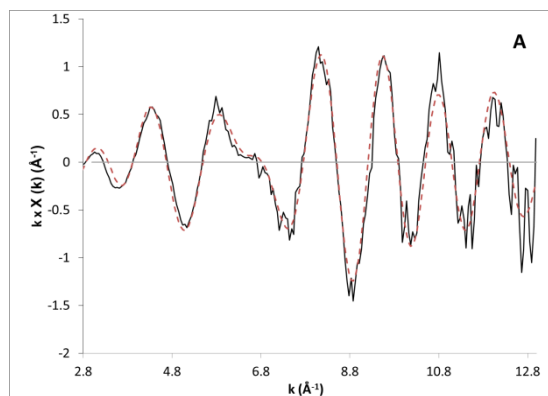


Fig. S11. EXAFS data recorded at the Rh K edge characterizing sample formed by adsorption of $\text{Rh}(\text{C}_2\text{H}_4)_2(\text{acac})$ on highly dehydroxylated MgO after treatment in H_2 for 1 h at 298 K and 1 bar (Table 1, sample 1): (A) k^1 -Weighted EXAFS function, $k^1(\chi)$ (solid line) and sum of the calculated contributions (dashed line). (B) k^1 -Weighted imaginary part and magnitude of the Fourier transform of data (solid line) and sum of the calculated contributions (dashed line). (C) k^3 -Weighted imaginary part and magnitude of the Fourier transform of data (solid line) and sum of the calculated contributions (dashed line). (D) k^1 -Weighted, phase- and amplitude-corrected, imaginary part and magnitude of the Fourier transform of data (solid line) and calculated contributions (dashed line) of Rh–C_{ethylene} shell. (E) k^1 -Weighted, phase- and amplitude-corrected, imaginary part and magnitude of the Fourier transform of data (solid line) and calculated contributions (dashed line) of Rh–O_{support} shell. (F) k^3 -Weighted, phase- and amplitude-corrected, imaginary part and magnitude of the Fourier transform of data (solid line) and calculated contributions (dashed line) of Rh–Mg shell. (G) k^3 -Weighted, phase- and amplitude-corrected, imaginary part and magnitude of the Fourier transform of data (solid line) and calculated contributions (dashed line) of Rh–Rh shell ($\Delta k = 3.5\text{--}12.5 \text{ \AA}^{-1}$). The approximate experimental uncertainties are as follows: coordination number N , $\pm 20\%$; R , $\pm 0.02 \text{ \AA}$; $\Delta\sigma^2$, $\pm 20\%$; and ΔE_0 , $\pm 20\%$ (but see the caveat stated above on page SI-3). The EXAFS data were fitted with 16 free parameters.



continued on next page

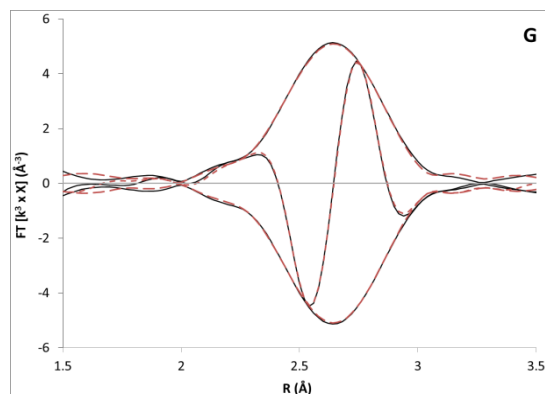
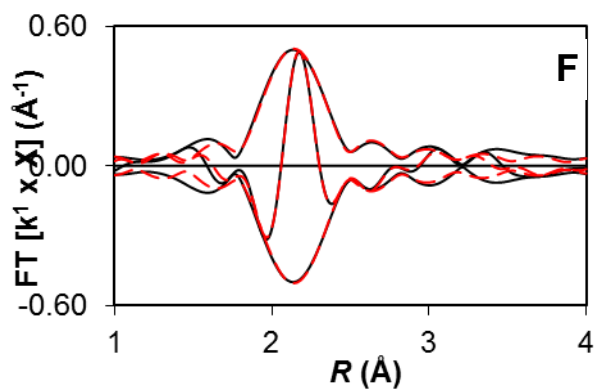
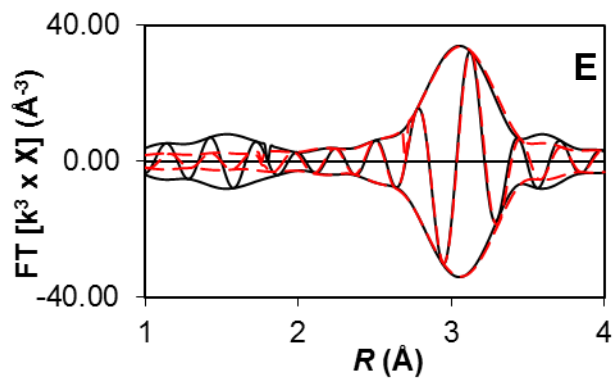
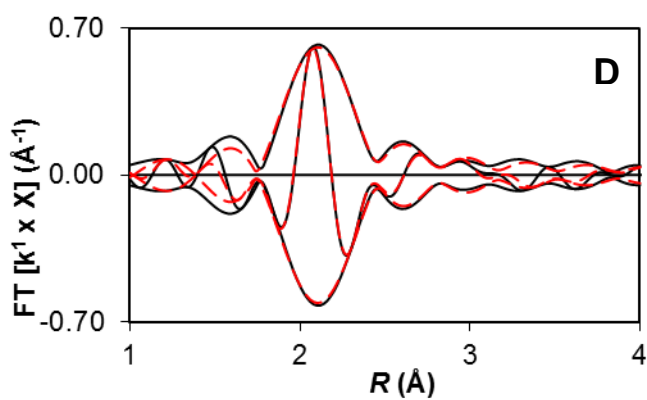
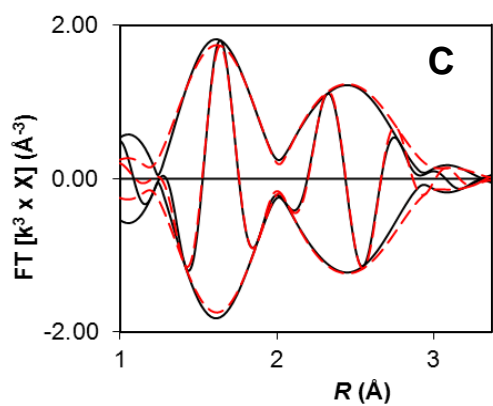
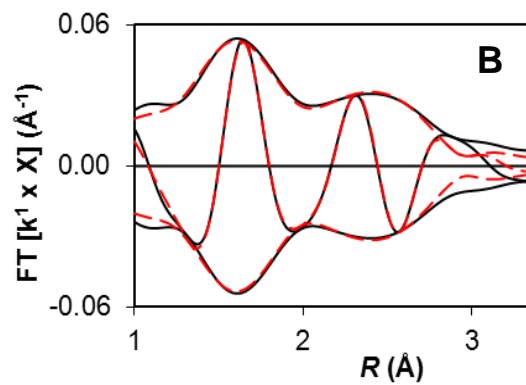
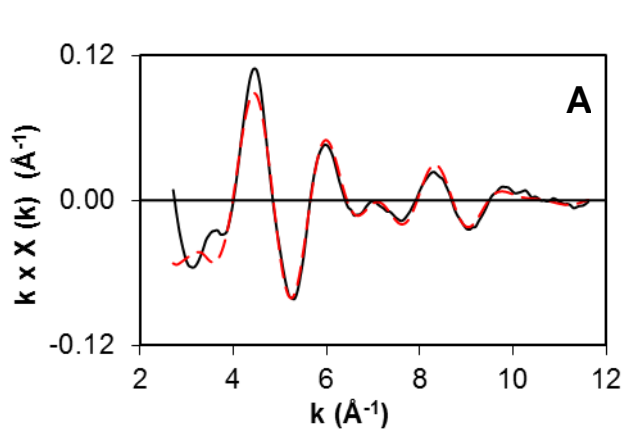


Fig. S12. EXAFS data recorded at the Rh K edge characterizing sample formed by adsorption of $\text{Rh}(\text{C}_2\text{H}_4)_2(\text{acac})$ on zeolite HY after treatment in H_2 for 1.5 h at 298 K and 1 bar (Table 1, sample 2): (A) k^1 -Weighted EXAFS function, $k^1(\chi)$ (solid line) and sum of the calculated contributions (dashed line). (B) k^1 -Weighted imaginary part and magnitude of the Fourier transform of data (solid line) and sum of the calculated contributions (dashed line). (C) k^3 -Weighted imaginary part and magnitude of the Fourier transform of data (solid line) and sum of the calculated contributions (dashed line). (D) k^1 -Weighted, phase- and amplitude-corrected, imaginary part and magnitude of the Fourier transform of data (solid line) and calculated contributions (dashed line) of Rh–C_{ethylene} shell. (E) k^1 -Weighted, phase- and amplitude-corrected, imaginary part and magnitude of the Fourier transform of data (solid line) and calculated contributions (dashed line) of Rh–O_{support} shell. (F) k^3 -Weighted, phase- and amplitude-corrected, imaginary part and magnitude of the Fourier transform of data (solid line) and calculated contributions (dashed line) of Rh–Al shell. (G) k^3 -Weighted, phase- and amplitude-corrected, imaginary part and magnitude of the Fourier transform of data (solid line) and calculated contributions (dashed line) of Rh–Rh shell ($\Delta k = 2.8\text{--}13.0 \text{ \AA}^{-1}$). The approximate experimental uncertainties are as follows: coordination number N , $\pm 20\%$; R , $\pm 0.02 \text{ \AA}$; $\Delta\sigma^2$, $\pm 20\%$; and ΔE_0 , $\pm 20\%$ (but see the caveat stated above on page SI-3). The EXAFS data were fitted with 16 free parameters.



continued on next page

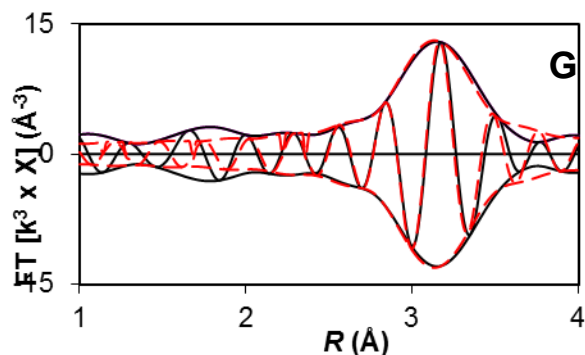
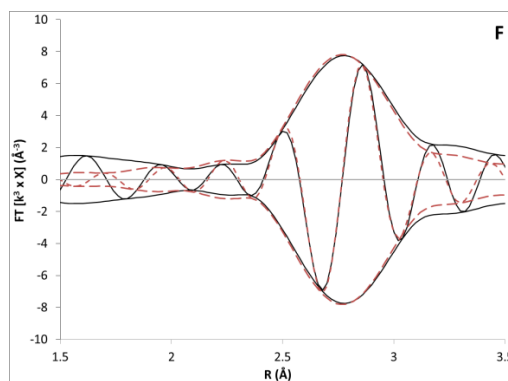
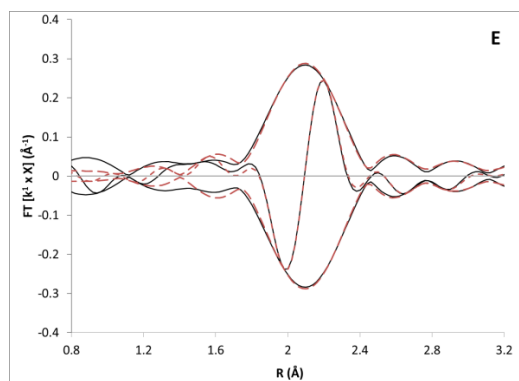
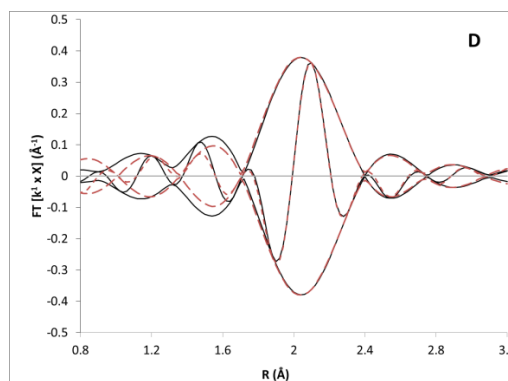
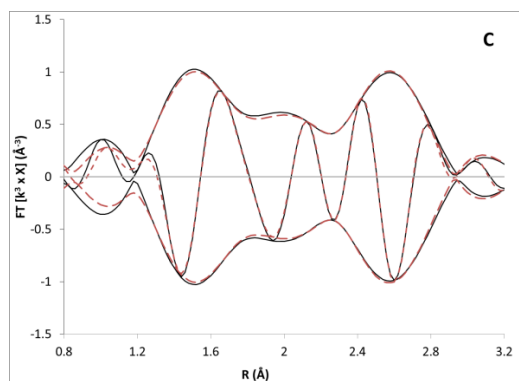
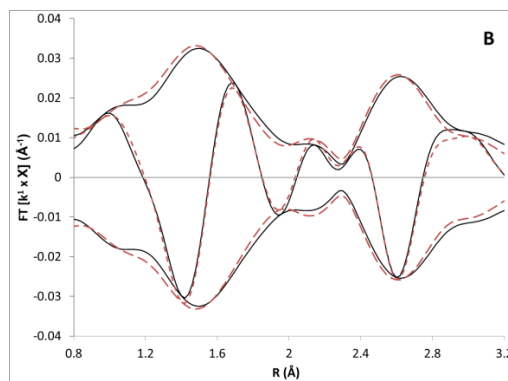
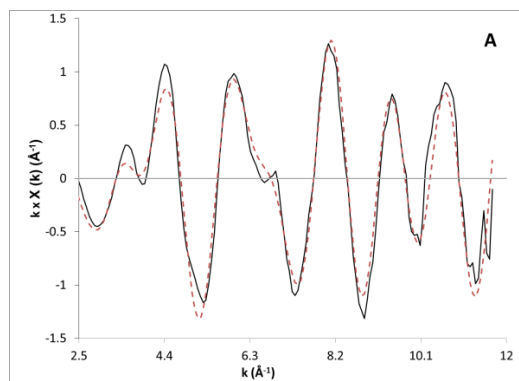


Fig. S13. EXAFS data recorded at the Rh K edge characterizing sample formed by adsorption of $\text{Rh}(\text{C}_2\text{H}_4)_2(\text{acac})$ on highly dehydroxylated MgO after the following treatments: 1) with a pulse of CO at 298 K and 1 bar to form $\text{Rh}(\text{CO})_2$ species on MgO; 2) in H_2 for 1 h at 298 K and 1 bar (Table 1, sample 3): (A) k^1 -Weighted EXAFS function, $k^1(\chi)$ (solid line) and sum of the calculated contributions (dashed line). (B) k^1 -Weighted imaginary part and magnitude of the Fourier transform of data (solid line) and sum of the calculated contributions (dashed line). (C) k^3 -Weighted imaginary part and magnitude of the Fourier transform of data (solid line) and sum of the calculated contributions (dashed line). (D) k^1 -Weighted, phase- and amplitude-corrected, imaginary part and magnitude of the Fourier transform of data (solid line) and calculated contributions (dashed line) of Rh- $\text{C}_{\text{COterminal}}$ shell. (E) k^3 -Weighted, phase- and amplitude-corrected, imaginary part and magnitude of the Fourier transform of data (solid line) and calculated contributions (dashed line) of Rh- $\text{O}_{\text{COterminal}}$ shell. (F) k^1 -Weighted, phase- and amplitude-corrected, imaginary part and magnitude of the Fourier transform of data (solid line) and calculated contributions (dashed line) of Rh- $\text{O}_{\text{support}}$ shell. (G) k^3 -Weighted, phase- and amplitude-corrected, imaginary part and magnitude of the Fourier transform of data (solid line) and calculated contributions (dashed line) of Rh-Mg shell ($\Delta k = 2.7\text{--}11.6 \text{ \AA}^{-1}$). The approximate experimental uncertainties are as follows: coordination number N , $\pm 20\%$; R , $\pm 0.02 \text{ \AA}$; $\Delta\sigma^2$, $\pm 20\%$; and ΔE_0 , $\pm 20\%$ (but see the caveat stated above on page SI-3). The EXAFS data were fitted with 15 free parameters, taking into account that the Rh- O_{CO} and the Rh- C_{CO} coordination numbers (referring to the oxygen atom and to carbon atom, respectively, of a carbonyl ligand) must be the same.



continued on next page

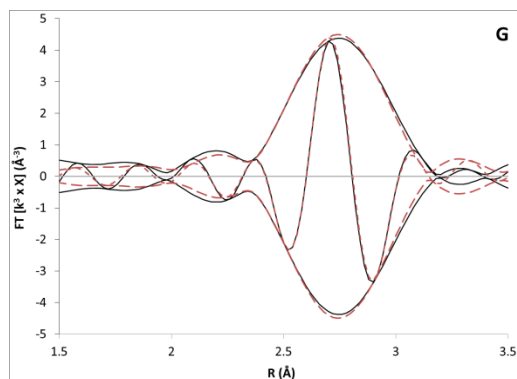


Fig. S14. EXAFS data recorded at the Rh K edge characterizing sample formed by adsorption of $\text{Rh}(\text{C}_2\text{H}_4)_2(\text{acac})$ on highly dehydroxylated MgO after 1 hour treatment in H_2 at 353 K and 1 bar (Table 1, sample 4): (A) k^1 -Weighted EXAFS function, $k^1(\chi)$ (solid line) and sum of the calculated contributions (dashed line). (B) k^1 -Weighted imaginary part and magnitude of the Fourier transform of data (solid line) and sum of the calculated contributions (dashed line). (C) k^3 -Weighted imaginary part and magnitude of the Fourier transform of data (solid line) and sum of the calculated contributions (dashed line). (D) k^1 -Weighted, phase- and amplitude-corrected, imaginary part and magnitude of the Fourier transform of data (solid line) and calculated contributions (dashed line) of Rh– $\text{C}_{\text{ethylene}}$ shell. (E) k^1 -Weighted, phase- and amplitude-corrected, imaginary part and magnitude of the Fourier transform of data (solid line) and calculated contributions (dashed line) of Rh– $\text{O}_{\text{support}}$ shell. (F) k^3 -Weighted, phase- and amplitude-corrected, imaginary part and magnitude of the Fourier transform of data (solid line) and calculated contributions (dashed line) of Rh–Mg shell. (G) k^3 -Weighted, phase- and amplitude-corrected, imaginary part and magnitude of the Fourier transform of data (solid line) and calculated contributions (dashed line) of Rh–Rh shell ($\Delta k = 2.5\text{--}11.7 \text{ \AA}^{-1}$). The approximate experimental uncertainties are as follows: coordination number N , $\pm 20\%$; R , $\pm 0.02 \text{ \AA}$; $\Delta\sigma^2$, $\pm 20\%$; and ΔE_0 , $\pm 20\%$ (but see the caveat stated above on page SI-3). The EXAFS data were fitted with 16 free parameters.

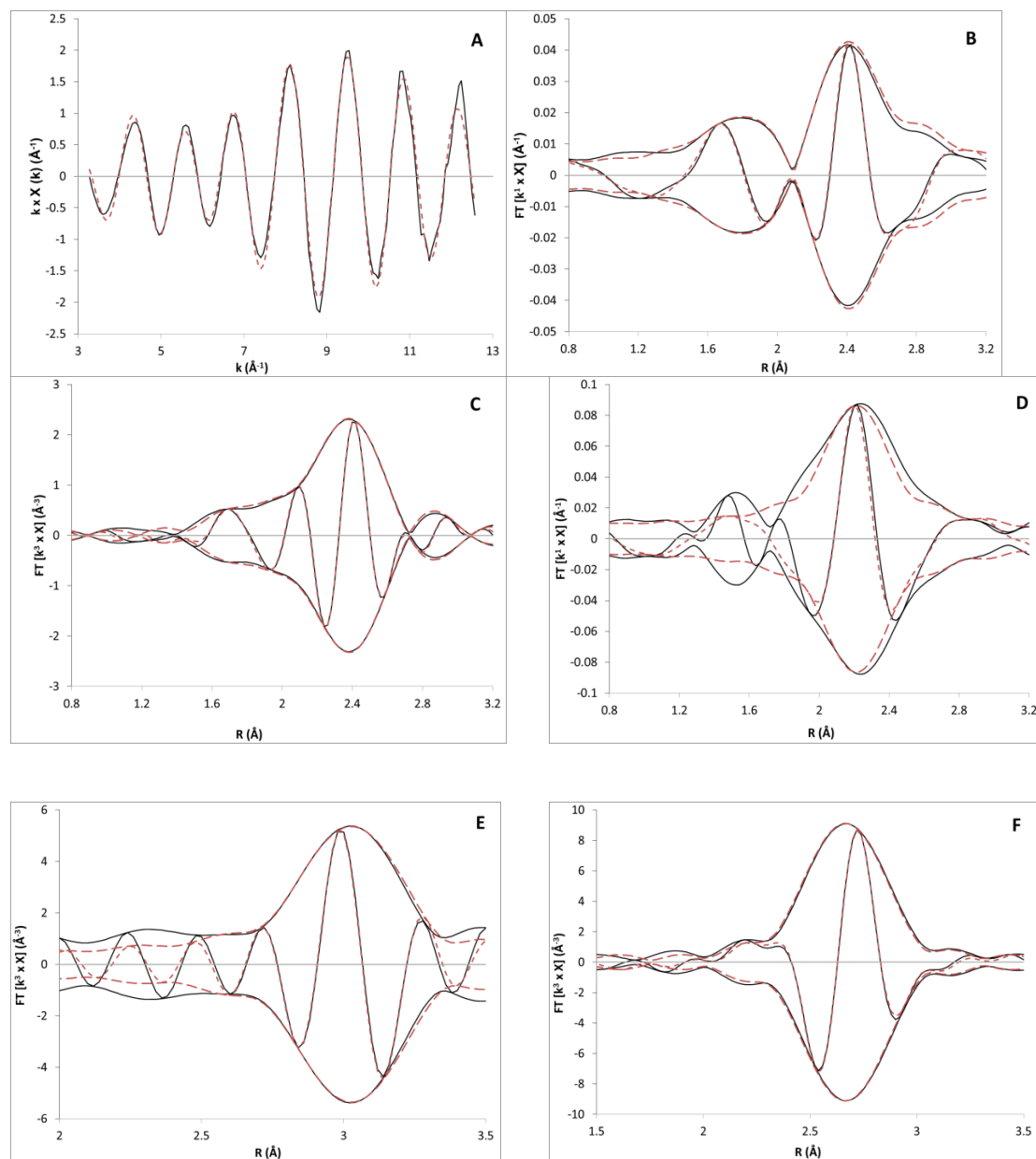
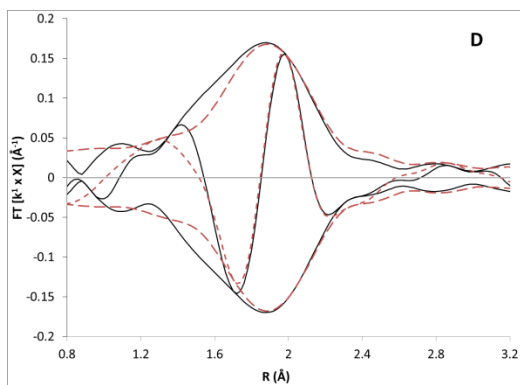
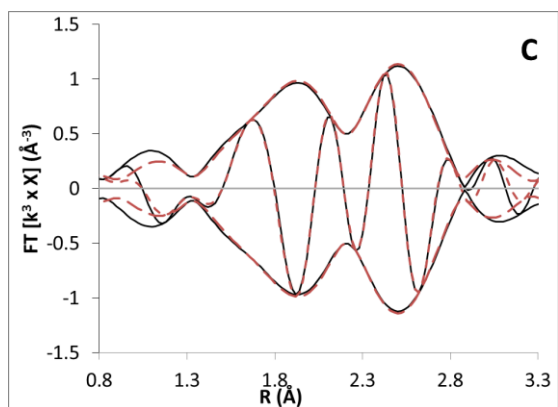
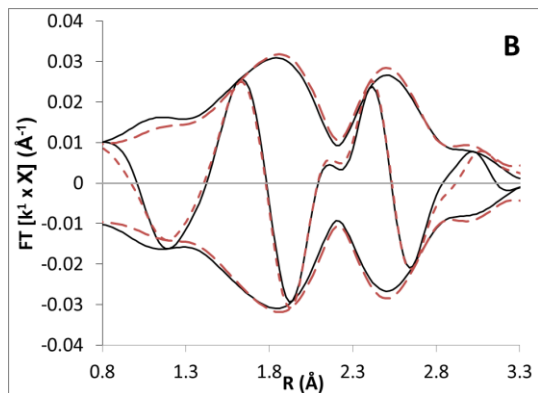
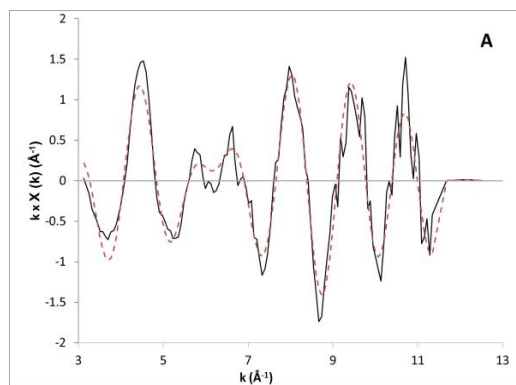


Fig. S15. EXAFS data recorded at the Rh K edge characterizing sample formed by adsorption of $\text{Rh}(\text{C}_2\text{H}_4)_2(\text{acac})$ on zeolite HY after 1 hour treatment in H_2 at 353 K and 1 bar (Table 1, sample 5): (A) k^1 -Weighted EXAFS function, $k^1(\chi)$ (solid line) and sum of the calculated contributions (dashed line). (B) k^1 -Weighted imaginary part and magnitude of the Fourier transform of data (solid line) and sum of the calculated contributions (dashed line). (C) k^3 -Weighted imaginary part and magnitude of the Fourier transform of data (solid line) and sum of the calculated contributions (dashed line). (D) k^1 -Weighted, phase- and amplitude-corrected, imaginary part and magnitude of the Fourier transform of data (solid line) and calculated contributions (dashed line) of Rh– $\text{O}_{\text{support}}$ shell. (E) k^3 -Weighted, phase- and amplitude-corrected, imaginary part and magnitude of the Fourier transform of data (solid line) and calculated contributions (dashed line) of Rh–Mg shell. (F) k^3 -Weighted, phase- and amplitude-corrected, imaginary part and magnitude of the Fourier transform of data (solid line) and calculated contributions (dashed line) of Rh–Rh shell ($\Delta k = 3.5\text{--}12.5 \text{ \AA}^{-1}$). The approximate experimental uncertainties are as follows: coordination number N , $\pm 20\%$; R , $\pm 0.02 \text{ \AA}$; $\Delta\sigma^2$, $\pm 20\%$; and ΔE_0 , $\pm 20\%$ (but see the caveat stated above on page SI-3). The EXAFS data were fitted with 12 free parameters.



continued on next page

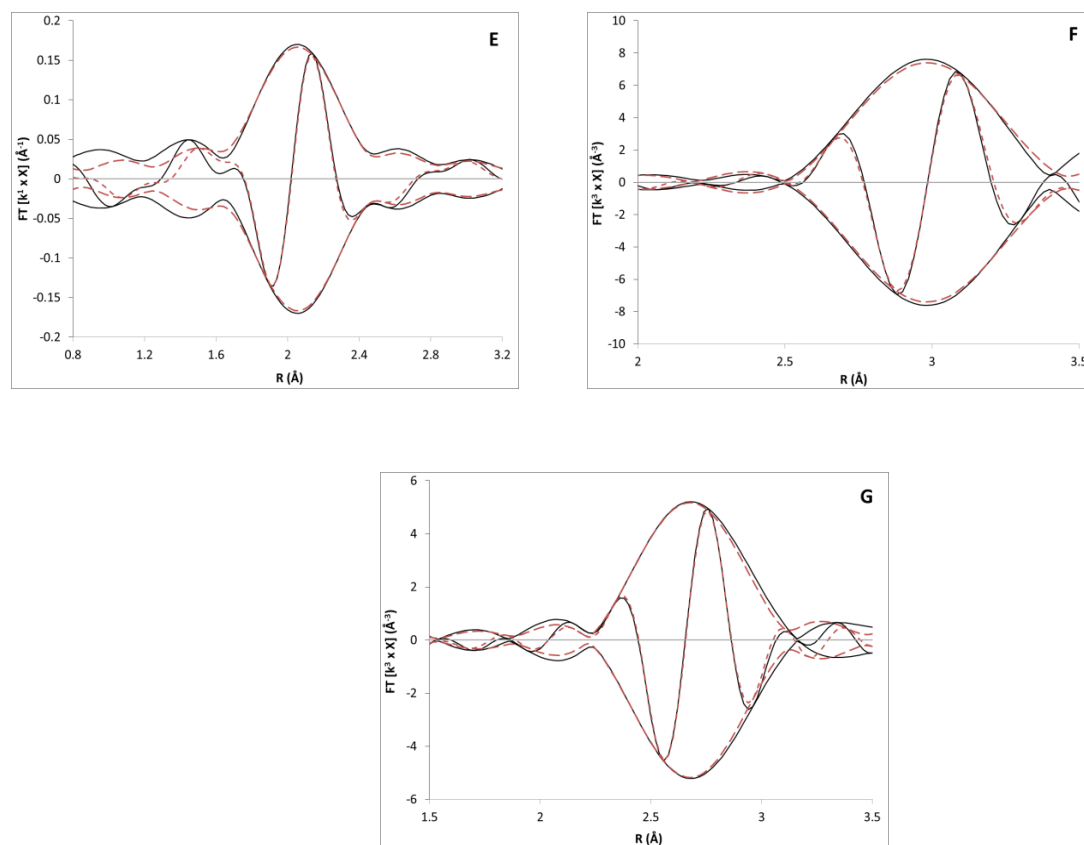
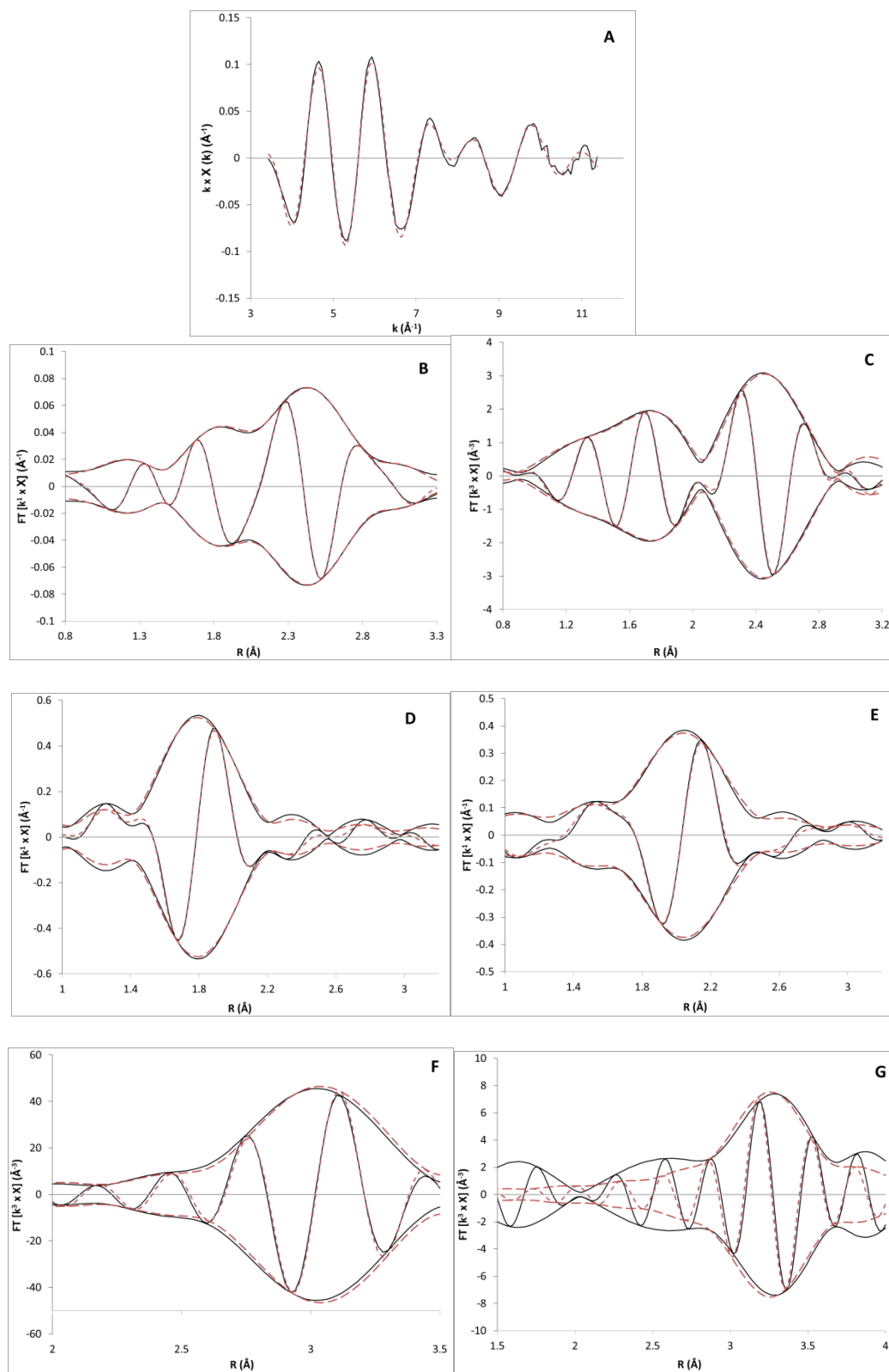
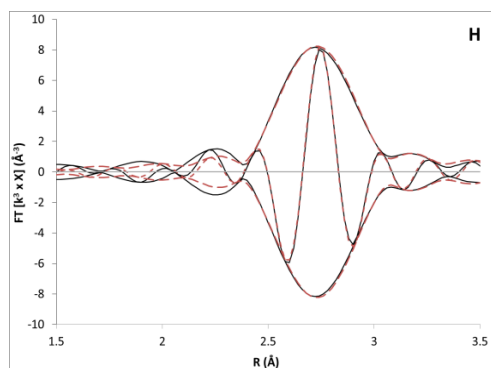
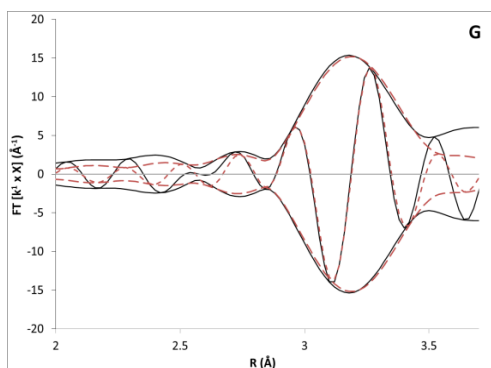
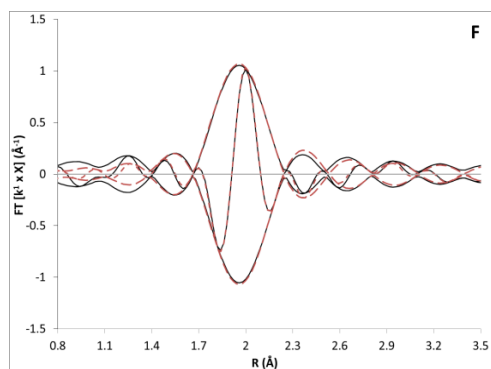
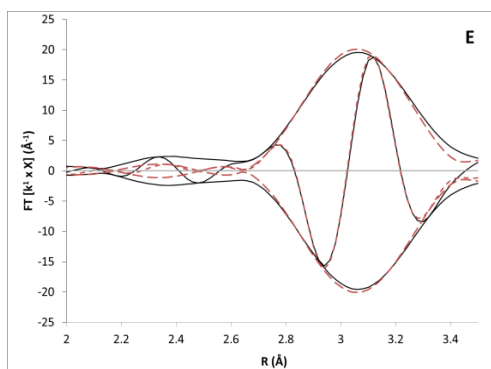
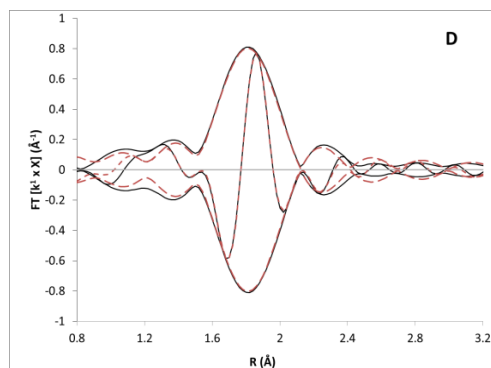
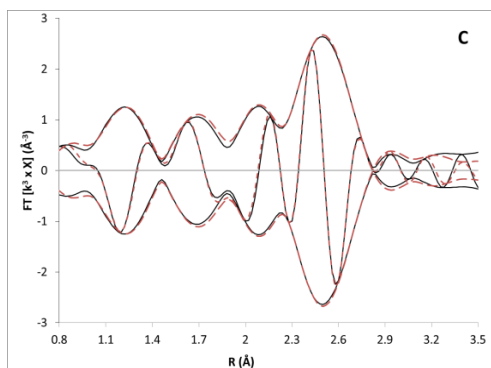
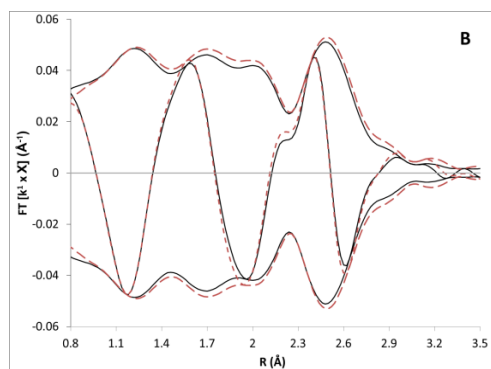
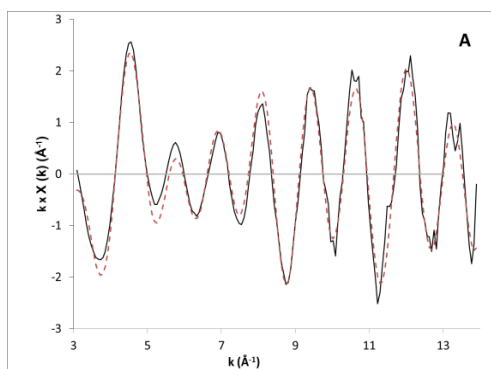


Fig. S16. EXAFS data recorded at the Rh K edge characterizing sample formed by adsorption of $\text{Rh}(\text{C}_2\text{H}_4)_2(\text{acac})$ on highly dehydroxylated MgO after the following treatments: 1) with a pulse of CO at 298 K and 1 bar to form $\text{Rh}(\text{CO})_2$ species on MgO; 2) in H_2 for 1 h at 393 K and 1 bar (Table 1, sample 6): (A) k^1 -Weighted EXAFS function, $k^1(\chi)$ (solid line) and sum of the calculated contributions (dashed line). (B) k^1 -Weighted imaginary part and magnitude of the Fourier transform of data (solid line) and sum of the calculated contributions (dashed line). (C) k^3 -Weighted imaginary part and magnitude of the Fourier transform of data (solid line) and sum of the calculated contributions (dashed line). (D) k^1 -Weighted, phase- and amplitude-corrected, imaginary part and magnitude of the Fourier transform of data (solid line) and calculated contributions (dashed line) of Rh–C_{carbonyl} shell. (E) k^1 -Weighted, phase- and amplitude-corrected, imaginary part and magnitude of the Fourier transform of data (solid line) and calculated contributions (dashed line) of Rh–O_{support} shell. (F) k^3 -Weighted, phase- and amplitude-corrected, imaginary part and magnitude of the Fourier transform of data (solid line) and calculated contributions (dashed line) of Rh–O_{carbonyl} shell. (G) k^3 -Weighted, phase- and amplitude-corrected, imaginary part and magnitude of the Fourier transform of data (solid line) and calculated contributions (dashed line) of Rh–Rh shell ($\Delta k = 3.2$ – 11.4 \AA^{-1}). The approximate experimental uncertainties are as follows: coordination number N , $\pm 20\%$; R , $\pm 0.02 \text{ \AA}$; $\Delta\sigma^2$, $\pm 20\%$; and ΔE_0 , $\pm 20\%$ (but see the caveat stated above on page SI-3). The EXAFS data were fitted with 15 free parameters, taking into account that the Rh–O_{CO} and the Rh–C_{CO} coordination numbers (referring to the oxygen atom and to carbon atom, respectively, of a carbonyl ligand) must be the same.



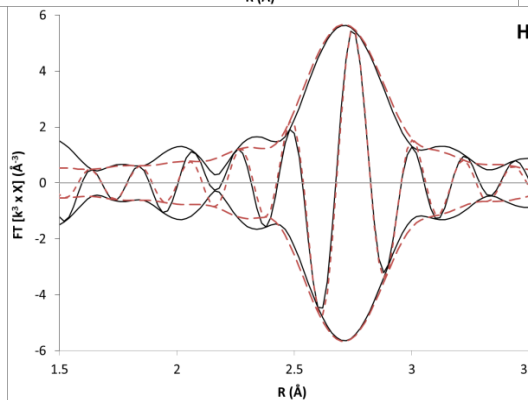
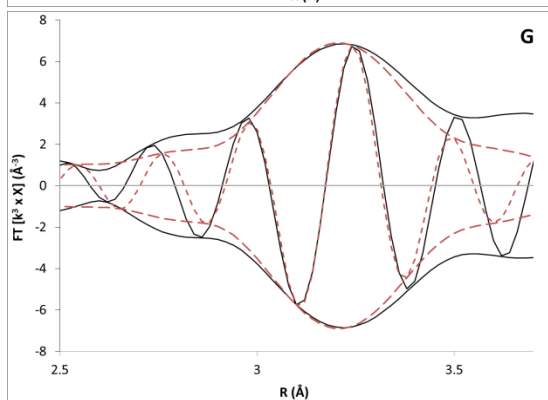
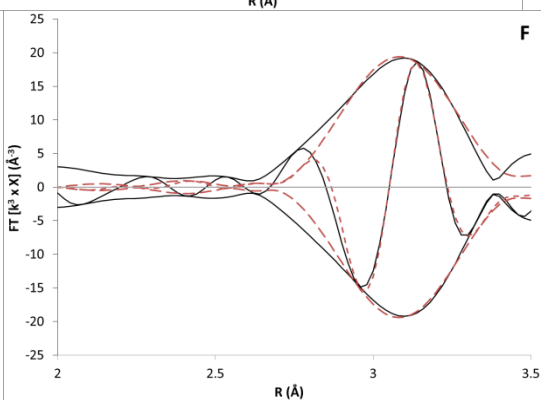
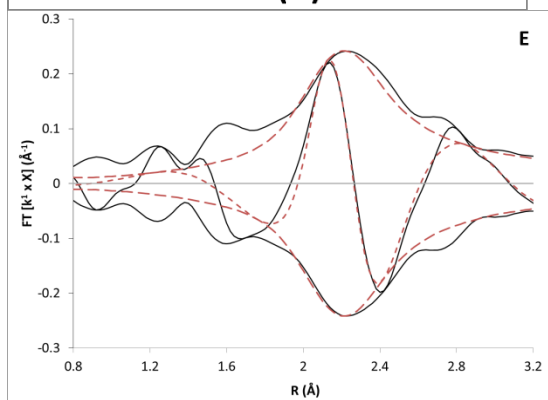
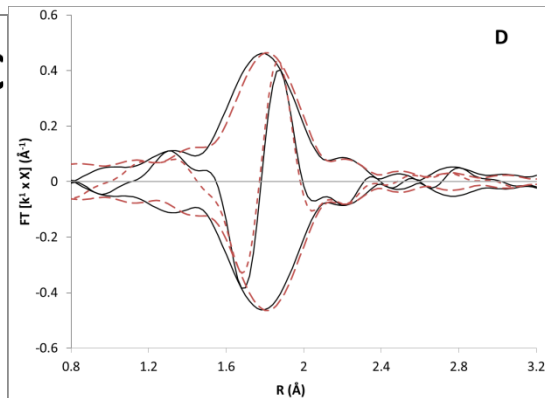
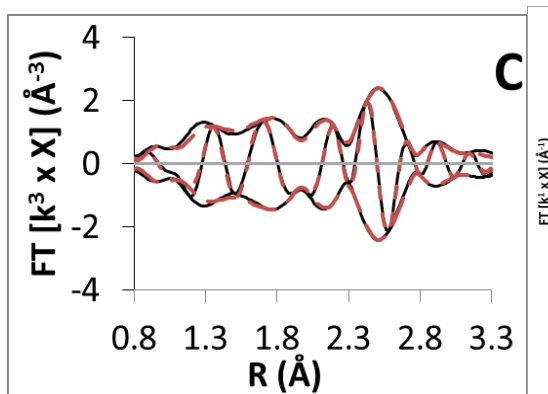
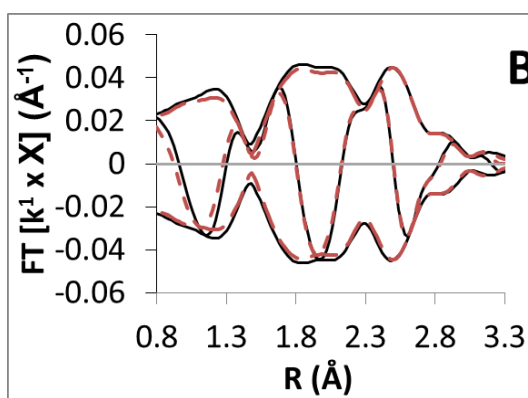
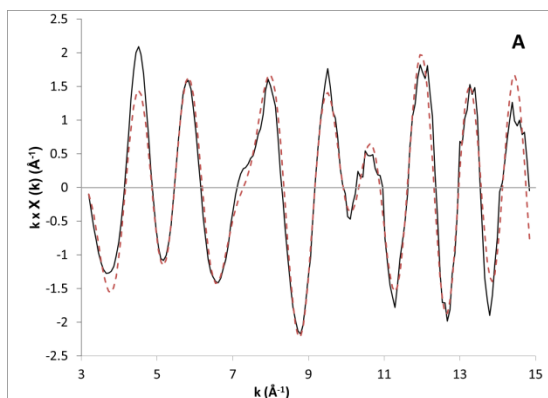
continued on next page

Fig. S17. EXAFS data recorded at the Rh K edge characterizing sample formed by adsorption of $\text{Rh}(\text{C}_2\text{H}_4)_2(\text{acac})$ on the zeolite HY after the following treatments: 1) with a pulse of CO at 298 K and 1 bar to form $\text{Rh}(\text{CO})_2$ species on zeolite HY; 2) in H_2 for 1 h at 423 K and 1 bar (Table 1, sample 7): (A) k^1 -Weighted EXAFS function, $k^1(\chi)$ (solid line) and sum of the calculated contributions (dashed line). (B) k^1 -Weighted imaginary part and magnitude of the Fourier transform of data (solid line) and sum of the calculated contributions (dashed line). (C) k^3 -Weighted imaginary part and magnitude of the Fourier transform of data (solid line) and sum of the calculated contributions (dashed line). (D) k^1 -Weighted, phase- and amplitude-corrected, imaginary part and magnitude of the Fourier transform of data (solid line) and calculated contributions (dashed line) of Rh-C_{CO} shell. (E) k^1 -Weighted, phase- and amplitude-corrected, imaginary part and magnitude of the Fourier transform of data (solid line) and calculated contributions (dashed line) of Rh-O_{support} shell. (F) k^1 -Weighted, phase- and amplitude-corrected, imaginary part and magnitude of the Fourier transform of data (solid line) and calculated contributions (dashed line) of Rh-O_{CO} shell. (G) k^3 -Weighted, phase- and amplitude-corrected, imaginary part and magnitude of the Fourier transform of data (solid line) and calculated contributions (dashed line) of Rh-Al shell ($\Delta k = 3.4\text{--}11.4 \text{ \AA}^{-1}$). The approximate experimental uncertainties are as follows: coordination number N , $\pm 20\%$; R , $\pm 0.02 \text{ \AA}$; $\Delta\sigma^2$, $\pm 20\%$; and ΔE_0 , $\pm 20\%$ (but see the caveat stated above on page SI-3). The EXAFS data were fitted with 15 free parameters, taking into account that the Rh-O_{CO} and the Rh-C_{CO} coordination numbers (referring to the oxygen atom and to carbon atom, respectively, of a carbonyl ligand) must be the same.



continued on next page

Fig. S18. EXAFS data recorded at Rh K edge characterizing the supported sample prepared by adsorption of $\text{Rh}(\text{C}_2\text{H}_4)_2(\text{acac})$ on highly dehydroxylated MgO after the following sequence of treatments: 1) in H_2 for 1 h at 353 K and 1 bar; 2) CO pulse at 298 K and 1 bar; (Table 1, sample 8): (A) k^1 -Weighted EXAFS function, $k^1(\chi)$ (solid line) and sum of the calculated contributions (dashed line). (B) k^1 -Weighted imaginary part and magnitude of the Fourier transform of data (solid line) and sum of the calculated contributions (dashed line). (C) k^3 -Weighted imaginary part and magnitude of the Fourier transform of data (solid line) and sum of the calculated contributions (dashed line). (D) k^1 -Weighted, phase- and amplitude-corrected, imaginary part and magnitude of the Fourier transform of data (solid line) and calculated contributions (dashed line) of Rh- $\text{C}_{\text{COterminal}}$ shell. (E) k^1 -Weighted, phase- and amplitude-corrected, imaginary part and magnitude of the Fourier transform of data (solid line) and calculated contributions (dashed line) of Rh- $\text{O}_{\text{COterminal}}$ shell. (F) k^1 -Weighted, phase- and amplitude-corrected, imaginary part and magnitude of the Fourier transform of data (solid line) and calculated contributions (dashed line) of Rh- $\text{C}_{\text{CObridging}}$ shell. (G) k^1 -Weighted, phase- and amplitude-corrected, imaginary part and magnitude of the Fourier transform of data (solid line) and calculated contributions (dashed line) of Rh- $\text{O}_{\text{CObridging}}$ shell. (H) k^3 -Weighted, phase- and amplitude-corrected, imaginary part and magnitude of the Fourier transform of data (solid line) and calculated contributions (dashed line) of Rh-Rh shell ($\Delta k = 3.1\text{--}13.8 \text{ \AA}^{-1}$). The approximate experimental uncertainties are as follows: coordination number N , $\pm 20\%$; R , $\pm 0.02 \text{ \AA}$; $\Delta\sigma^2$, $\pm 20\%$; and ΔE_0 , $\pm 20\%$ (but see the caveat stated above on page SI-3). The EXAFS data were fitted with 20 free parameters.



continued from preceding page

Fig. S19. EXAFS data recorded at Rh K edge characterizing the supported sample prepared by adsorption of $\text{Rh}(\text{C}_2\text{H}_4)_2(\text{acac})$ on zeolite HY after the following sequence of treatments: 1) in H_2 for 1 h at 353 K and 1 bar; 2) CO pulse at 298 K and 1 bar; (Table 1, sample 9): (A) k^1 -Weighted EXAFS function, $k^1(\chi)$ (solid line) and sum of the calculated contributions (dashed line). (B) k^1 -Weighted imaginary part and magnitude of the Fourier transform of data (solid line) and sum of the calculated contributions (dashed line). (C) k^3 -Weighted imaginary part and magnitude of the Fourier transform of data (solid line) and sum of the calculated contributions (dashed line). (D) k^1 -Weighted, phase- and amplitude-corrected, imaginary part and magnitude of the Fourier transform of data (solid line) and calculated contributions (dashed line) of Rh- $\text{C}_{\text{Cterminal}}$ shell. (E) k^1 -Weighted, phase- and amplitude-corrected, imaginary part and magnitude of the Fourier transform of data (solid line) and calculated contributions (dashed line) of Rh- $\text{O}_{\text{support}}$ shell. (F) k^1 -Weighted, phase- and amplitude-corrected, imaginary part and magnitude of the Fourier transform of data (solid line) and calculated contributions (dashed line) of Rh- $\text{O}_{\text{Cterminal}}$ shell. (G) k^3 -Weighted, phase- and amplitude-corrected, imaginary part and magnitude of the Fourier transform of data (solid line) and calculated contributions (dashed line) of Rh-Al shell. (H) k^3 -Weighted, phase- and amplitude-corrected, imaginary part and magnitude of the Fourier transform of data (solid line) and calculated contributions (dashed line) of Rh-Rh shell ($\Delta k = 3.2\text{--}14.8 \text{ \AA}^{-1}$). The approximate experimental uncertainties are as follows: coordination number N , $\pm 20\%$; R , $\pm 0.02 \text{ \AA}$; $\Delta\sigma^2$, $\pm 20\%$; and ΔE_0 , $\pm 20\%$ (but see the caveat stated above on page SI-3). The EXAFS data were fitted with 20 free parameters.

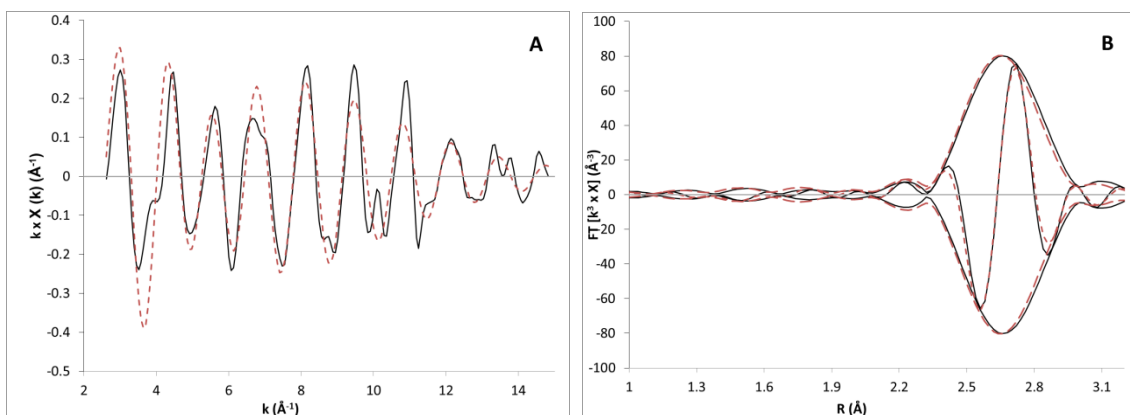


Fig. S20. EXAFS data recorded at Rh K edge characterizing the Rh foil; (Table S2): (A) k^1 -Weighted EXAFS function, $k^1(\chi)$ (solid line) and sum of the calculated contributions (dashed line). (B) k^3 -Weighted imaginary part and magnitude of the Fourier transform of data (solid line) and sum of the calculated contributions (dashed line). ($\Delta k = 2.6$ – 14.8 \AA^{-1}). The approximate experimental uncertainties are as follows: coordination number N , $\pm 20\%$; R , $\pm 0.02 \text{ \AA}$; $\Delta\sigma^2$, $\pm 20\%$; and ΔE_0 , $\pm 20\%$ (but see the caveat stated above on page SI-3). The EXAFS data were fitted with 4 free parameters.

1 M. Newville, *J. Synchrotron Rad.* 2001, **8**, 322

2 M. Vaarkamp, J. C. Linders, D. C. Koningsberger, *Physica B* 1995, **209**, 159

3 a) P. S. Kirilin, F. B. M. van Zon, D. C. Koningsberger, B. C. Gates, *J. Phys. Chem. B* 1990, **94**, 8439; b) J. B. A. D. van Zon, D.C. Koningsberger, H. F. J. van't Blik, D. E. Sayers, *J. Chem. Phys.* 1985, **82**, 5742; c) J. Guzman, B. C. Gates, *J. Catal.* 2004, **226**, 111

4 S. I. Zabinsky, J. J. Rehr, A. Ankudinov, R. C. Albers, M. J. Eller, *Phys. Rev. B.* 1995, **52**, 2995

5 International XAFS Society, Error Reporting Recommendations: A Report of the Standards and Criteria Committee. http://fisica.unicam.it/IXS/OLD/subcommittee_reports/sc/err-rep.pdf (accessed Feb 2006).

6 F.W. Lytle, D. E. Sayers, E. A. Stern, *Physica B* 1989, **158**, 701